

The Low-Energy Fixed Points of Random Quantum Spin Chains

E. Westerberg,* A. Furusaki,† M. Sigrist,‡ and P. A. Lee

Department of Physics, Massachusetts Institute of Technology, Cambridge, Massachusetts 02139

The one-dimensional isotropic quantum Heisenberg spin systems with random couplings and random spin sizes are investigated using a real-space renormalization group scheme. It is demonstrated that these systems belong to a universality class of disordered spin systems, characterized by weakly coupled large effective spins. In this large-spin phase the uniform magnetic susceptibility diverges as T^{-1} with a non-universal Curie constant at low temperatures T , while the specific heat vanishes as $T^\delta |\ln T|$ for $T \rightarrow 0$. For broad range of initial distributions of couplings and spin sizes the distribution functions approach a single fixed-point form, where $\delta \approx 0.44$. For some singular initial distributions, however, fixed-point distributions have non-universal values of δ , suggesting that there is a line of fixed points.

I. INTRODUCTION

Over many decades one-dimensional (1D) quantum spin systems ('quantum spin chains') have attracted a lot of interest and led to the development of many theoretical methods which are now commonly used for the study of other highly correlated systems.¹ Despite the apparent simplicity of quantum spin chains, they show a wealth of physical properties which give a key to our understanding of various phenomena, e.g., quantum phase transitions, topological order, and fractional statistics.^{1–3} Since the discovery of various quasi-1D materials, the study of 1D spin systems, which is mainly based on the Heisenberg model and its variations, is also of experimental relevance. Examples of such materials include so-called NINO, NENP,^{4,5} and $\text{Sr}_3\text{CuPtO}_6$.⁶ In particular, the latter system belongs to a class of compounds which is compositionally very flexible and has been under intense experimental investigation over the last few years. This type of quasi-1D system was first reported in Sr_4PtO_6 by Randall and Katz,⁷ and it is now possible to produce compounds of the form Sr_3MNO_6 in various combinations with $\text{M} = \text{Cu}, \text{Mg}, \text{Zn}, \text{Yb}, \text{Na}, \text{Ca}, \text{Co}$ and $\text{N} = \text{Pt}, \text{Ir}, \text{Rh}, \text{Bi}$.

Disorder effects play a particularly important role in 1D quantum spin systems, as even small deviations from the regular system often destabilize the pure phases.⁸ Real experimental systems naturally contain impurities and other types of disorder. Therefore it is very important to understand the influence of disorder on the properties of such systems in order to interpret experimental results. To our knowledge, the first 1D spin system recognized for its disorder belongs to the class of charge-transfer salts TCNQ (tetracyanoquinodimethane).⁹ These systems have been successfully described by a 1D spin- $\frac{1}{2}$ Heisenberg model with random strength of antiferromagnetic exchange couplings between the spins. A more recent example of disordered spin chains is $\text{Sr}_3\text{CuPt}_{1-x}\text{Ir}_x\text{O}_6$.¹⁰ While the pure compounds $\text{Sr}_3\text{CuPtO}_6$ ($x = 0$) and $\text{Sr}_3\text{CuIrO}_6$ ($x = 1$) are antiferromagnetic (AF) and ferromagnetic (FM) spin systems, respectively, the alloy $\text{Sr}_3\text{CuPt}_{1-x}\text{Ir}_x\text{O}_6$ contains both AF and FM couplings. The fraction of FM bonds is simply related to x , the concentration of Ir ions. In a previous work, we modeled $\text{Sr}_3\text{CuPt}_{1-x}\text{Ir}_x\text{O}_6$ with a nearest-neighbor spin- $\frac{1}{2}$ Heisenberg chain, where the exchange coupling between neighboring spins is $+J$ or $-J$ with probability p and $1 - p$ respectively. The methods we used (high-temperature expansion and transfer matrix approximation) give reliable results down to $k_B T \sim J/5$, where T is the temperature and k_B is Boltzmann's constant. In this regime the numerically calculated magnetic susceptibility $\chi(T)$ and the specific heat $C(T)$ interpolate smoothly between the corresponding quantities of purely FM ($p = 1$) and AF ($p = 0$) chains, giving good qualitative agreement with experimental data.^{11,12} At temperatures below $\sim J/k_B$ the effects of disorder become significant. We demonstrated that in this temperature regime spins correlate within AF and FM segments of the chain separately. The emerging new degrees of freedom which dominate the thermodynamics are (large) effective spins each corresponding to a correlated segment. The size of these spins and their residual interaction are set by the local disorder and hence is random. From exact diagonalization of finite segments we concluded that the low-temperature physics of the random spin system is described by the effective Hamiltonian,

$$\mathcal{H} = \sum_i J_i \mathbf{S}_i \cdot \mathbf{S}_{i+1} , \quad (1)$$

where both the couplings J_i , which may have either sign, and the spin sizes S_i are random. In particular, we emphasize that the resulting distribution of J_i in Eq. (1) is broad and dense, in contrast to the discrete distribution of the initial

model. In this paper we take Eq. (1) as starting point. We discuss the low-temperature properties of this model, and the various fixed points encountered for different initial distributions of couplings and spins.¹³

Before going into details we briefly summarize our results and the method we use, which is a generalization of the RSRG scheme introduced by Ma, Dasgupta and Hu (MDH) in 1979 to study the 1D spin- $\frac{1}{2}$ random antiferromagnet (RAF).¹⁴ The RAF, where all couplings are antiferromagnetic but vary in magnitude, has also been investigated using Kadanoff block spin RG techniques,¹⁵ and more recently by the density matrix RG method.¹⁶ The method of Dasgupta *et al.* has proven to be the most successful one, and was recently extended by Fisher,¹⁷ who solved the RG equations exactly.

In the MDH RSRG scheme, a decimation of degrees of freedom occurs through the successive formation of spin singlets from the most strongly coupled spin pairs. This scheme conserves the form of the Hamiltonian in the original model, but changes the distribution of couplings, which gradually approaches a fixed-point form. The model in Eq. (1) contains arbitrary spin sizes and couplings with random sign, so that, in general, two correlated spins do not combine into a singlet. Rather they form an effective spin with renormalized couplings to its neighbors. Here we introduce a modified RSRG scheme which takes this into account. Like the MDH RSRG scheme it conserves the form of the Hamiltonian, Eq. (1), but changes the distributions of couplings and gaps. The RG flow generated can therefore be thought of as a flow in the space of distributions of couplings and gaps.¹⁸ We demonstrate that for a wide range of initial distributions of couplings and spins, the RG flow of the distribution functions eventually approaches a single universal fixed point. This fixed point represents the following physical properties. Both entropy and specific heat vanish as $T^{2\alpha}|\ln T|$, where the power $\alpha \approx 0.22$ is rather small. The exponent α appears also in the non-linear magnetization where $M(H) \propto H^{\alpha/1+\alpha}$ for sufficiently large fields H . For very singular initial distribution of the couplings we find that α takes a non-universal value, suggesting the presence of a fixed line. We also find a surprising fact that, for both the universal and non-universal fixed points, the susceptibility follows the Curie behavior down to zero temperature with a non-universal Curie constant. We finally show how the two previously known random phases, the random singlet phase (RSP) and the random dimer solid (RDS)^{19,20}, both of which correspond to Eq. (1) with all $S_i = 1/2$ and all $J_i > 0$, are unstable against the admixture of an arbitrarily small concentration of FM couplings and/or larger spins.

Our paper has the following structure. We start with a brief review of the MDH RSRG scheme in Sec. II A, before we generalize it to chains with both AF and FM couplings in Sec. II B. In Sec. III we analyze the distributions of spins and couplings, and their scaling forms close to a fixed point. We perform the RG scheme numerically by simulating random spin chains with various initial distributions of couplings and spins. The numerical results shown in Sec. IV confirm the scaling forms conjectured in Sec. III, but also reveal that random spin chains with very singular initial distributions of gaps flow to non-universal fixed points. In Sec. V we derive the scaling forms of thermodynamic quantities, and in Sec. VI we comment on the approximations involved in the RG transformation. Finally we summarize our results in Sec. VII, and compare the large-spin phase (LSP) to other disordered phases. We also discuss the stability of the various phases and in particular the RG flow between the LSP, RSP, and RDS.

II. THE RENORMALIZATION-GROUP SCHEME

To study the low-temperature properties of systems described by Eq. (1), we generalize a RSRG method introduced by Ma, Dasgupta and Hu (MDH).¹⁴ We start with a brief review of the MDH scheme for the RAF with $S_i = 1/2$ and random $J_i > 0$.

A. The MDH RG for antiferromagnetic spin- $\frac{1}{2}$ chains

Consider an antiferromagnetic nearest-neighbor Heisenberg spin- $\frac{1}{2}$ chain in which the largest coupling is J_0 and the remaining couplings J_i are distributed according to $P(J_0; J_i)$. We focus on the link with the largest coupling, $J_i = J_0$, and the terms in the Hamiltonian (1) that involve the spins \mathbf{S}_i and \mathbf{S}_{i+1} , (see Fig. 1a),

$$\mathcal{H}' = \mathcal{H}'_0 + \mathcal{H}'_I \quad (2)$$

where

$$\begin{aligned} \mathcal{H}'_0 &= J_0 \mathbf{S}_i \cdot \mathbf{S}_{i+1} , \\ \mathcal{H}'_I &= J_{i-1} \mathbf{S}_{i-1} \cdot \mathbf{S}_i + J_{i+1} \mathbf{S}_{i+1} \cdot \mathbf{S}_{i+2} . \end{aligned}$$

If the distribution $P(J_0; J)$ is broad, $J_{i\pm 1}$ are typically much smaller than J_0 and we can treat \mathcal{H}'_I as a perturbation to \mathcal{H}'_0 . In the ground state of \mathcal{H}'_0 the spins \mathbf{S}_i and \mathbf{S}_{i+1} form a singlet, and the energy gap to the excited states is J_0 . This ground state is four-fold degenerate since the unperturbed Hamiltonian \mathcal{H}'_0 does not involve the directions of \mathbf{S}_{i-1} and \mathbf{S}_{i+2} . \mathcal{H}'_I lifts the degeneracy and splits the unperturbed ground state into a singlet and a triplet, and the low energy spectrum of the four-spin Hamiltonian (2) is described by an effective Hamiltonian

$$\mathcal{H}^{\text{eff}} = \tilde{J} \mathbf{S}_{i-1} \cdot \mathbf{S}_{i+2} . \quad (3)$$

The effective coupling \tilde{J} is determined from the energy splitting of the unperturbed ground state, and to second order in $J_{i\pm 1}/J_0$ the result is $\tilde{J}/J_0 = \frac{J_{i-1}J_{i+1}}{2J_0^2}$. Physically the weak interaction between \mathbf{S}_{i-1} and \mathbf{S}_{i+2} is mediated by exciting virtual triplet states in the interjacent spin pair.

In the Hamiltonian (1) we replace the terms in \mathcal{H}' with the effective interaction \mathcal{H}^{eff} in Eq. (3) to get an effective Hamiltonian for the low-energy degrees of freedom of the spin chain. Repeating this procedure and successively replacing the strongest remaining coupling in the chain preserves the form of the Hamiltonian but changes the distribution of couplings and, in particular, lowers J_0 , the largest remaining coupling in the chain. If $P(J'_0, J)$ is the distribution of couplings at a point when the largest remaining coupling is J'_0 , then the removal of bonds $J_i \in [J_0 - dJ_0, J_0]$ generates a flow equation for $P(J_0, J)$ ¹⁴

$$\frac{dP(J_0; J)}{dJ_0} = -P(J_0; J_0) \int_0^{J_0} dJ_1 dJ_2 P(J_0; J_1) P(J_0; J_2) \delta(J - J_1 J_2 / 2J_0) . \quad (4)$$

The flow equation (4) is derived under the assumption that there are no spatial correlations among the bond strengths. This is indeed the case if there are no correlations in the distribution of couplings in the initial chain. It has been shown that if the initial distribution of bonds is normalizable, Eq. (4) has a unique fixed-point solution that governs the low-energy physics of random bond antiferromagnetic spin- $\frac{1}{2}$ chains.^{17,21}

B. Generalization of the MDH RG

We apply the same strategy to the random spin chain with couplings of either sign and random spin sizes. In contrast to the previous case, a link is determined not only by the coupling strength but also by its left and right spin, $\{\Delta_i, S_i, S_{i+1}\}$ (see Fig. 1b). We define Δ_i as the energy gap between the ground state multiplet and the first excited multiplet in the corresponding two-spin Hamiltonian $\mathcal{H} = J_i \mathbf{S}_i \cdot \mathbf{S}_{i+1}$:²²

$$\Delta_i = \begin{cases} |J_i|(S_i + S_{i+1}) & : J_i < 0 \text{ (ferromagnetic link)} , \\ J_i(|S_i - S_{i+1}| + 1) & : J_i > 0 \text{ (antiferromagnetic link)} . \end{cases} \quad (5)$$

We assume a broad distribution of interaction energies and focus on the link in the chain which, if completely isolated from the rest of the chain, requires the largest energy $\Delta = \Delta_0$ to excite the ground state multiplet. We consider the situation illustrated in Fig. 1c, where $\{\Delta_0, S_L, S_R\}$ is the strongest link in the chain, and $\{\Delta_1, S_1, S_L\}$ and $\{\Delta_2, S_R, S_2\}$ are its adjacent links. In the spirit of the MDH RSRG scheme we replace the strongest link $\{\Delta_0, S_L, S_R\}$ with an effective spin of size $S = |S_L \pm S_R|$ representing the lowest-energy multiplet of maximum (minimum) spin for a ferromagnetic (antiferromagnetic) link. The residual effective interaction for \mathbf{S}_1 , \mathbf{S} , and \mathbf{S}_2 is calculated perturbatively in $\varepsilon_{1,2} = \Delta_{1,2}/\Delta_0$. The effective interaction is isotropic, and to first order in $\varepsilon_{1,2}$ given by

$$\mathcal{H}^{\text{eff}} = \tilde{J}_1 \mathbf{S}_1 \cdot \mathbf{S} + \tilde{J}_2 \mathbf{S} \cdot \mathbf{S}_2 \quad (6)$$

with

$$J_0 > 0, J_1 > 0, S_L > S_R \implies \tilde{\Delta}_1 = \Delta_1 f_1(S_1, S_L, S_R); \tilde{J}_1 > 0 \quad (7a)$$

$$J_0 > 0, J_1 > 0, S_L < S_R \implies \tilde{\Delta}_1 = \Delta_1 f_2(S_1, S_L, S_R); \tilde{J}_1 < 0 \quad (7b)$$

$$J_0 > 0, J_1 < 0, S_L > S_R \implies \tilde{\Delta}_1 = \Delta_1 f_3(S_1, S_L, S_R); \tilde{J}_1 < 0 \quad (7c)$$

$$J_0 > 0, J_1 < 0, S_L < S_R \implies \tilde{\Delta}_1 = \Delta_1 f_4(S_1, S_L, S_R); \tilde{J}_1 > 0 \quad (7d)$$

$$J_0 < 0, J_1 > 0 \implies \tilde{\Delta}_1 = \Delta_1 f_5(S_1, S_L, S_R); \tilde{J}_1 > 0 \quad (7e)$$

$$J_0 < 0, J_1 < 0 \implies \tilde{\Delta}_1 = \Delta_1 f_6(S_1, S_L, S_R); \tilde{J}_1 < 0 \quad (7f)$$

where

$$f_1(S_1, S_L, S_R) = \frac{(S_L + 1)(|S_1 - S_L + S_R| + 1)}{(S_L - S_R + 1)(|S_1 - S_L| + 1)} \quad (8a)$$

$$f_2(S_1, S_L, S_R) = \frac{S_L(S_1 + S_R - S_L)}{(S_R - S_L + 1)(|S_1 - S_L| + 1)} \quad (8b)$$

$$f_3(S_1, S_L, S_R) = \frac{(S_L + 1)(S_1 + S_L - S_R)}{(S_L - S_R + 1)(S_1 + S_L)} \quad (8c)$$

$$f_4(S_1, S_L, S_R) = \frac{S_L(|S_1 - S_R + S_L| + 1)}{(S_R - S_L + 1)(S_1 + S_L)} \quad (8d)$$

$$f_5(S_1, S_L, S_R) = \frac{S_L(|S_1 - S_L - S_R| + 1)}{(S_L + S_R)(|S_1 - S_L| + 1)} \quad (8e)$$

$$f_6(S_1, S_L, S_R) = \frac{S_L(S_1 + S_L + S_R)}{(S_L + S_R)(S_1 + S_L)} . \quad (8f)$$

A derivation of these equations is shown in Appendix A 1. From the knowledge of the gap $\tilde{\Delta}_1$ and the sign of \tilde{J}_1 , \tilde{J}_1 is readily calculated via Eq. (5). Similarly $\tilde{\Delta}_2$ is obtained by replacing S_1 by S_2 and S_L by S_R in Eqs. (7) and (8). These equations do not require the spins to be multiples of $1/2$, and from now on we regard spins as continuous variables. The case where the strongest link is antiferromagnetic with $S_L = S_R$ is not accounted for in Eq. (7). In this case the two spins S_L and S_R form a singlet, and the leading order contribution to the effective coupling between S_1 and S_2 is (c.f. Appendix A 2)

$$\tilde{J} = \frac{2J_1 J_2}{3J_0} S_L(S_L + 1) , \quad (9)$$

which is easily translated into $\tilde{\Delta}$ via Eq. (5). For $S_L = S_R = 1/2$ this is the original MDH RG transformation.

As in the original RSRG scheme, the effect of successively forming effective spins is to change the distributions of gaps and spins (links) without changing the form of the Hamiltonian. In analogy to the probability distribution for the couplings in the RAF, we define probability distributions of ferromagnetic (P^F) and antiferromagnetic (P^A) links where the largest remaining gap in the chain is Δ_0 ,

$$P^F(\Delta_0; \Delta, S_L, S_R) , \quad (10a)$$

$$P^A(\Delta_0; \Delta, S_L, S_R) . \quad (10b)$$

The probability distributions $P^{A,F}$ are symmetric in S_L and S_R and obey the normalization condition

$$\int_0^{\Delta_0} d\Delta \int_0^\infty dS_L dS_R [P^F(\Delta_0; \Delta, S_L, S_R) + P^A(\Delta_0; \Delta, S_L, S_R)] = 1 , \quad (11)$$

for any value of Δ_0 . From P^A and P^F we can calculate the distributions of spins, gaps and coupling constants. As a special case, the original spin- $\frac{1}{2}$ antiferromagnetic chain studied in Ref. 14 corresponds to

$$P^A(\Delta_0; \Delta, S_L, S_R) = \delta(S_L - \frac{1}{2})\delta(S_R - \frac{1}{2})P(\Delta_0; \Delta) , \quad (12a)$$

$$P^F(\Delta_0; \Delta, S_L, S_R) = 0 . \quad (12b)$$

If there are no correlations between neighboring links (except for the obvious correlation that they share one spin), the flow equations for $P^{A,F}$ are

$$\frac{dP^A}{d\Delta_0} = F_1[P^A, P^F] , \quad (13a)$$

$$\frac{dP^F}{d\Delta_0} = F_2[P^A, P^F] , \quad (13b)$$

which generalize the MDH RSRG flow equation (4). In Eqs. (13) F_1 and F_2 are two (non-linear) functionals of P^A and P^F , whose explicit forms depend on the functions f_n in Eq. (8), c.f. Appendix B.

III. SCALING FORMS OF THE PROBABILITY DISTRIBUTIONS

As links are replaced by effective spins, the effective couplings and, hence, the gaps of the links decrease. At the same time the average distance na_0 between neighboring effective spins as well as the magnitude of the effective spins increase. (Here a_0 is the original lattice constant and n is the ratio of the number of original spins to the number of effective spins.) We expect that the link distributions eventually approach a fixed point where P^A , P^F and n exhibit scaling behavior

$$P^A(\Delta_0; \Delta, S_L, S_R) = \Delta_0^{-\gamma_A} Q^A \left(\frac{\Delta}{\Delta_0^{\beta_A}}, \frac{S_L}{\Delta_0^{-\alpha_A}}, \frac{S_R}{\Delta_0^{-\alpha_A}} \right) , \quad (14a)$$

$$P^F(\Delta_0; \Delta, S_L, S_R) = \Delta_0^{-\gamma_F} Q^F \left(\frac{\Delta}{\Delta_0^{\beta_F}}, \frac{S_L}{\Delta_0^{-\alpha_F}}, \frac{S_R}{\Delta_0^{-\alpha_F}} \right) , \quad (14b)$$

and

$$n \sim \Delta_0^{-\delta} . \quad (15)$$

The exponent δ is related to the dynamical exponent z ($z = 1/\delta$). The seven exponents in Eqs. (14) and (15) are not all independent. Indeed, we argue below that

$$\alpha_F = \alpha_A \equiv \alpha \quad (16a)$$

$$\beta_F = \beta_A = 1 \quad (16b)$$

$$\gamma_F = \gamma_A = 1 - 2\alpha \quad (16c)$$

$$\delta = 2\alpha \quad (16d)$$

so that in the scaling regime

$$P^A = \frac{1}{\Delta_0^{1-2\alpha}} Q^A(\Delta/\Delta_0, S_L \Delta_0^\alpha, S_R \Delta_0^\alpha) \quad (17a)$$

$$P^F = \frac{1}{\Delta_0^{1-2\alpha}} Q^F(\Delta/\Delta_0, S_L \Delta_0^\alpha, S_R \Delta_0^\alpha) \quad (17b)$$

with length scaling as

$$n \sim \Delta_0^{-2\alpha} . \quad (18)$$

The relations (16) have been confirmed in numerical simulations (*c.f.* Sec. IV) and can be understood as follows.

Let $x = N_A/(N_A + N_F)$ be the fraction of AF links in the chain. Both FM ($x = 0$) and AF ($x = 1$) chains are unstable towards a small concentration of couplings of the opposite sign. To see that $x = 1$ is unstable, we note that unless the effective spin formed is a singlet, the removal of a link in an AF chain converts one neighboring link into a FM link. Similarly $x = 0$ is unstable because an isolated AF link in a FM environment always survives (the removal of a FM link does not change the signs of its neighboring links, and if the AF link itself is removed, one of its FM neighbors is converted into an AF link). This implies that for small enough x the absolute number of AF links is constant, so that the fraction x of AF links increases as links are removed. Thus, unless we start with a completely FM random spin chain or a purely AF random spin chain with uniform magnitude of the spins, the fixed-point distribution contains both FM and AF links. Having established that both x_0 and $1 - x_0$, the fraction of AF and FM links at the fixed point respectively, are non-zero, we can easily derive the relations (16a-c). Since a finite fraction of the spins belong to both a FM and an AF link, there cannot be a separation in scales between spin sizes in AF and FM links, i.e., $\alpha_A = \alpha_F = \alpha$. $\beta_F = 1$ ($\beta_A = 1$) follows from the fact that the average gap in the FM (AF) distribution, when measured in units of Δ_0 is finite and independent of Δ_0 . $\gamma_A = 1 - 2\alpha$ follows trivially from the finiteness of x_0

$$\begin{aligned} x_0 &= \int_0^{\Delta_0} d\Delta \int_0^\infty dS_L dS_R \Delta_0^{-\gamma_A} Q^A(\Delta/\Delta_0, \Delta_0^\alpha S_L, \Delta_0^\alpha S_R) \\ &= \Delta_0^{1-2\alpha-\gamma_A} \int_0^1 d\Delta' \int_0^\infty ds' ds'' Q^A(\Delta', s', s'') , \end{aligned} \quad (19)$$

which must be independent of Δ_0 . An analogous argument for $1 - x_0$ implies $\gamma_F = 1 - 2\alpha$.

The last relation (16d) requires a more detailed analysis of the way effective spins are formed by correlating the original spins in clusters. The size of the effective spin corresponds to the spin quantum number of the ground state of the cluster. Since the spin system is not frustrated the spin quantum number is determined from the classical correlation of the spins (parallel and antiparallel). The total spin of a cluster of n spins is then given by

$$S = \left| \sum_{i=1}^n \pm S_i \right| , \quad (20)$$

where two neighboring spins enter the sum with the same (opposite) sign if their mutual coupling is ferromagnetic (antiferromagnetic). This leads to a typical random walk problem which results in the scaling

$$S \sim n^{1/2} . \quad (21)$$

From this we conclude $\delta = 2\alpha$.

The remaining independent exponent, which we take to be α , is related to the average renormalization of the gaps. Consider two neighboring effective spins with a coupling corresponding to a gap Δ . Suppose also that each of the two effective spins is made up of 2^k spins at some larger energy scale Δ' . As the energy scale is lowered from Δ' to Δ and the 2^k spins form one large effective spin, the gap Δ is typically renormalized $2k$ times (k times in the course of formation of the left effective spin and similarly k times from the right). If the magnitude of a gap is reduced on average by a factor a each time a neighboring link is replaced with an effective spin, then

$$n \sim n' 2^k = n' (a^{2k})^{\frac{1}{2 \ln a}} \sim n' \left(\frac{\Delta}{\Delta'} \right)^{\frac{\ln 2}{2 \ln a}} , \quad (22)$$

from which we read off the relation

$$\alpha = -\frac{\ln 2}{4 \ln a} . \quad (23)$$

Using the scaling form, we can get some information on long-distance behavior of spin-spin correlation functions. Let us introduce two kinds of spin-spin correlation functions which characterizes the correlation between spins at low temperatures. The first one is the usual spin-spin correlation function,

$$C_1(i - j) = \langle \mathbf{S}_i \cdot \mathbf{S}_j \rangle , \quad (24)$$

where $\langle \rangle$ represents both thermal average and average over random configurations. Since the number of AF bonds between \mathbf{S}_i and \mathbf{S}_j is random, the two spins may either be in parallel or antiparallel. Thus, after taking the random average the correlation function decays exponentially for large $|i - j|$ even at zero temperature:

$$C_1(i - j) \propto \exp \left\{ -|i - j| \left[\ln \left(\frac{1}{|2p - 1|} \right) + i\pi\Theta(1 - 2p) \right] \right\} , \quad (25)$$

where p is the density of FM bonds. Therefore this correlation function does not reflect the correlations leading to the formation of effective large spins. An appropriate correlation function is

$$C_2(i - j) = \langle \eta_{ij} \mathbf{S}_i \cdot \mathbf{S}_j \rangle , \quad (26)$$

where $\eta_{ij} = \prod_{k=i}^{j-1} \text{sgn}(-J_k)$ for $j > i$. At finite temperature this correlation function should also decay exponentially for large $|i - j|$ with the correlation length n :

$$C_2(i - j) \propto \exp(-|i - j|/n) \quad \text{for } T > 0. \quad (27)$$

From Eq. (18) we find that the correlation length grows with decreasing temperature as $n \propto T^{-2\alpha}$. It is likely that at zero temperature the correlation function decays algebraically as

$$C_2(i - j) \propto \frac{1}{|i - j|^\nu} . \quad (28)$$

Unfortunately we cannot determine the value of this new exponent ν from our numerical RG scheme.

IV. NUMERICAL RESULTS

We perform our RG scheme by numerical simulations. We start each simulation by generating a chain according to independent probability distributions for gaps and spins. In each decimation step we pick up the strongest link in the chain, replace it with an appropriate effective spin, and renormalize the neighboring bonds. To keep the number of links fixed, one site is finally added in one end of the chain. This procedure is then iterated until the shape of the distribution function of links no longer changes. In this way we have iterated sixteen chains with both non-singular and singular initial distribution, see Tab. I.

In all our simulations the distributions of links eventually converged to some fixed-point distributions. The distributions rather quickly take the rough forms of the fixed-point distributions, while the final approach and, in particular, the convergence of the exponents in Eqs. (16) to their final values are very slow and take place over up to five orders of magnitudes in length (ten orders of magnitude in energy). Our numerical simulations demonstrate that unless the initial distribution has a high degree of singularity for small gaps, the distribution of links in the chain eventually flows to a universal fixed-point distribution of AF and FM links. If the initial distribution of gaps is more singular than $P(\Delta) \sim \Delta^{-y_c}$, $y_c \approx 0.7$, our numerical simulations suggest that the corresponding fixed-point distribution is non-universal. This is analogous to the RAF where it has been shown that extremely singular components in the gap distribution are conserved in the RG flow.¹⁷ In the case of the RAF $y_c = 1$, so that the condition for a chain to flow to the universal fixed-point distribution coincides with normalizability. In contrast to the RAF, there may be physical situations where a random AF/FM spin chain flows to a non-universal fixed-point distribution,²⁰ c.f. Sec. VII. Below we summarize the numerical results in the case of regular and singular gap-distributions.

A. Regular and weakly singular distributions

If the initial distribution of gaps is regular or at least less singular than $P(\Delta) \sim \Delta^{-0.7}$, we find that the link-distributions in all chains we have studied (chains A, B, C, D, F, H, and I in Tab. I) eventually converge to the same universal distribution with the characteristic scaling form (17) proposed in section III. The fixed-point distribution functions are illustrated by various cross-sections in Figs. 2 and 3. We find that the ratio of AF links stabilizes around $x = 0.63$, thus confirming the conjecture in section III that both x_0 and $1 - x_0$ are non-zero. The exponents $\alpha_{A,F}$ and $\beta_{A,F}$ in Eqs. (14) are deduced from the scaling of the averages $\langle S \rangle$ and $\langle \Delta \rangle$ with Δ_0 in the scaling regime. This is illustrated in Fig. 4 for chain C in Tab. I, where the average gap and spin size are plotted versus Δ_0 in a log-log plot. Similarly the ratio n of the number of original spins to the number of effective spins is plotted versus the maximum gap Δ_0 in Fig. 4b, and the evolution of the exponents as functions of Δ_0 are plotted in Figs. 5a and 5b. We find the fixed-point values of the exponents to be

$$\begin{aligned}\alpha_{A,F} &= 0.22 \pm 0.01 , \\ \beta_{A,F} &= 1.00 \pm 0.005 , \\ \delta &= 0.44 \pm 0.02 .\end{aligned}$$

The exponents in the FM distribution agree with the ones in the AF distribution within numerical accuracy. Thus our numerical findings confirm the scaling forms (17) and (18) for the probability distributions of the links as well as the relations between the exponents, Eqs. (16). Identifying α with either α_A , α_F or $\frac{1}{2}\delta$ gives consistently

$$\alpha = 0.22 \pm 0.01 . \quad (29)$$

An interesting observation we have made is that the ratio $2\alpha/\delta$ generally stabilizes to its fixed-point value of 1 before the two exponents δ and α separately converge to their corresponding fixed-point values. This confirms the robustness of the ‘random walk’ argument in Sec. III leading to the relation in Eq. (16d).

The typical expansion parameters in the perturbative calculation of the renormalized gaps are the median ratios between $\Delta^{A,F}$ and Δ_0 . At the fixed point these ratios are

$$\begin{aligned}\Delta_t^A / \Delta_0 &\sim 0.2 , \\ \Delta_t^F / \Delta_0 &\sim 0.3 ,\end{aligned}$$

where we denote the median gap in the distributions of antiferromagnetic and ferromagnetic links by Δ_t^A and Δ_t^F respectively. As expected from the increase in effective spin size, the formation of a singlet on a link ($S_R = S_L$) becomes increasingly rare as the fixed point is approached.

B. Strongly singular distributions

For chains with a very singular initial distribution of gaps the convergence to some fixed-point distribution is generally even slower than for regular (or modestly singular) chains. Furthermore, in these cases the fixed-point distribution that is eventually approached as well as the scaling exponent appears to be non-universal. This is illustrated in Fig. 6, where the fixed-point distributions for four chains are plotted. The dotted distributions correspond to chains where the initial gap-distributions are $P(\Delta) \propto \Delta^{-x}$ with $x = \{3/4, 4/5, 7/8\}$ (Tab. I). The solid curve is the corresponding fixed-point distribution for regular chains discussed in Sec. IV A. For reasons discussed below, the actual form of the distributions corresponding to singular initial distributions may be quantitatively incorrect, but they deviate clearly from the fixed-point distribution of regular chains. Numerically we find that chains with initial gap-distribution more singular than

$$P(\Delta) \sim \Delta^{-y_c} \quad \text{with} \quad 0.65 \lesssim y_c \lesssim 0.75 \quad (30)$$

flow to non-universal fixed-point distributions. From log-log plots of the universal fixed point-distribution of gaps, Fig. 7, we find that the distribution of FM gaps diverges as $P^F(\Delta) \sim \Delta^{-0.44}$ and the distribution of AF gaps as $P^A(\Delta) \sim \Delta^{-0.70}$ for small gaps. Thus, even from a regular link-distribution the RG transformation itself produces a singular fixed-point distribution of gaps, where the degree of the singularity, $P(\Delta) \sim \Delta^{-y_c}$, is set by details in the RG transformation rather than by the initial conditions. If a distribution is more singular than Δ^{-y_c} , the singular component is conserved in the RG flow. This is supported by our numerical results that y_c in Eq. (30) is somewhere between 0.65 and 0.75, which agrees with the singularity in the universal fixed-point distribution of gaps $P(\Delta) \sim \Delta^{-0.70}$. We conjecture that in chains with gap-distributions more singular than Δ^{-y_c} , the low-energy fixed point is not determined by the RG transformation alone, but also by the singular distribution of extremely weak links. In these chains we expect the fixed-point distribution as well as the value of the scaling exponent to be non-universal.

The picture we present is in close analogy to the RAF where Fisher has shown that the flow equation (4) conserves very singular components of $P(\Delta_0, \Delta)$.¹⁷ In the case of the RAF $y_c = 1$, implying that any normalizable (and hence physical) initial distribution eventually flows to a universal fixed-point distribution.

The fact that a very singular fixed-point distribution is dominated by the weakest links in the initial chain casts some doubt on the numerical results for such chains at low energies. Indeed, since all our chains have only a finite number of links, the singularity cannot be resolved perfectly. Hence the number of initially extremely weak links which are important for the low-energy behavior of the chain are relatively few and we do not expect the numerical results for the extremely singular chains to be quantitatively correct. This explains why the singularity seems to soften at very low energies while we argue that it should remain constant. Still, the qualitative result that regular (or slightly singular) chains flow to a universal fixed-point distribution while more singular distributions do not, should be correct.

V. THERMODYNAMICS

A. Entropy and specific heat

The scaling forms in Eqs. (17) and (18) allow us to determine the universal temperature dependence of various thermodynamic quantities which may be measured in experiments. Let us start with the entropy and the specific heat. At finite temperature T the renormalization group flow stops at $\Delta_0 \sim k_B T$ due to thermal fluctuations which prevent the formation of even larger effective spins. At this point, all pairs of spins in links with gaps larger than $\Delta_0 \sim k_B T$ form large effective spins. Since the distribution of gaps is broad, the interaction energies between the effective spins are typically much smaller than $\Delta_0 \sim k_B T$, and each large spin moves essentially independently. The entropy per unit length is hence

$$\frac{\sigma(T, H = 0)}{L} \propto \frac{k_B \ln(2\langle S_{\text{eff}} \rangle + 1)}{n} \propto T^{2\alpha} |\ln T| \quad (31)$$

in the scaling regime where $\langle S_{\text{eff}} \rangle \gg 1$. Note that the assumption of independent effective spins leads to an overestimate of the entropy. From the relation $C(T) = T \frac{d\sigma}{dT}$ follows the specific heat per unit length

$$\frac{C(T, H = 0)}{L} \propto T^{2\alpha} |\ln T| . \quad (32)$$

This is qualitatively different than in the random spin- $\frac{1}{2}$ antiferromagnet where $\sigma(T) \propto |\ln T|^{-2}$. This is also in contrast to the uniform 1D antiferromagnet where $\sigma_{AF}(T) \propto T$ and the uniform ferromagnet, $\sigma_{FM}(T) \propto \sqrt{T}$. The fact that both the entropy and the specific heat of the random-exchange spin chains go to zero with a rather small power reflects the presence of large number of uncorrelated spin degrees of freedom at low temperature.

B. Static magnetic susceptibility

By analogous arguments, the essentially uncorrelated large effective spins give a Curie-like contribution to the magnetic susceptibility per unit length

$$\frac{\chi}{L} = \frac{\mu^2}{3k_B T} \frac{\langle S_{\text{eff}}^2 \rangle}{n} = \frac{c}{T} \frac{\Delta_0^{-2\alpha}}{\Delta_0^{-2\alpha}} = \frac{c}{T} . \quad (33)$$

The T^{-1} Curie behavior is usually a signature of uncorrelated spins. We emphasize that this is *not* the case for the random spin chain. Rather, most of the original spins are *strongly* correlated, and the Curie-like temperature dependence follows from the scaling relation $n \sim \langle S_{\text{eff}}^2 \rangle$, Eq. (21). The Curie constant c can be calculated in terms of the original spin distributions as follows. As discussed in Sec. III, the magnitude of the effective spin representing a segment of n frozen spins is given by the sum

$$S_{\text{eff}}^2 = \left(\sum_{i=1}^n \delta_i S_i \right)^2 , \quad (34)$$

where the staggering factor δ_i is defined by

$$\delta_{i+1} = -\delta_i \text{sgn}(J_i) \quad ; \quad \delta_1 = 1 \quad , \quad (35)$$

and $S_i > 0$ is the spin size of the elementary spin at site i . Averaging over the (initial) disorder, we obtain

$$\langle S_{\text{eff}}^2 \rangle = \langle \left(\sum_{i=1}^n \delta_i S_i \right)^2 \rangle = n \langle S_i^2 \rangle + \langle S_i \rangle^2 \sum_{i \neq j} \langle \delta_i \delta_j \rangle . \quad (36)$$

Defining p as the probability for a bond to be ferromagnetic and using $\langle \delta_i \delta_j \rangle = (2p - 1)^{|i-j|}$ we get

$$\langle S_{\text{eff}}^2 \rangle = n \left[\langle S_i^2 \rangle + \frac{2p-1}{1-p} \langle S_i \rangle^2 + \mathcal{O}\left(\frac{1}{n}\right) \right] , \quad (37)$$

and in the limit of small T (large n) we find the Curie constant to be

$$c = \frac{\mu^2}{3k_B} \left[\langle S_i^2 \rangle + \frac{2p-1}{1-p} \langle S_i \rangle^2 \right] . \quad (38)$$

This result coincides with the low-temperature susceptibility we obtain for the analogous classical spin chain.¹¹ Note that this low-temperature Curie constant is in general different from the high-temperature value

$$\tilde{c} = \frac{\mu^2}{3k_B} \langle S_i(S_i + 1) \rangle . \quad (39)$$

It follows that $c = \tilde{c}$ only if

$$\frac{1-p}{2p-1} = \langle S_i \rangle . \quad (40)$$

Thus, in the random spin chain we expect the magnetic susceptibility to cross over from one Curie-like behavior at high temperature ($T \geq J/k_B$) to a different Curie-like regime at low-temperature ($T \leq J/k_B$).

C. Magnetization at finite H

In a finite magnetic field H and at finite temperature T the RG flow is interrupted either by the thermal energy $k_B T$ or by the magnetic Zeeman energy $E_{ZM} = \mu \langle S_{\text{eff}} \rangle H$. If $k_B T \geq E_{ZM}$ the chain is dominated by thermal fluctuations and the magnetization is given by χH . If $k_B T \leq E_{ZM}$ the magnetic field drives the system away from the fixed point of zero magnetic field into a state of aligned effective spins where the magnetization eventually saturates. In this regime a non-zero magnetic field starts to align the effective spins at an energy scale $\Delta_0 \sim \mu \langle S_{\text{eff}} \rangle H$. With above scaling properties this means $\Delta_0 \sim H^{1/1+\alpha}$, so that the saturated magnetization per unit length becomes $M/L \sim \mu \langle S_{\text{eff}} \rangle / n \sim H^{\alpha/1+\alpha}$. The condition that the chain is not yet dominated by thermal fluctuations is $k_B T < \Delta_0 \sim H^{1/1+\alpha}$. Summarizing these arguments, we get

$$\frac{M(T, H)}{L} \propto \begin{cases} H^{\frac{\alpha}{1+\alpha}} & : T^{1+\alpha} \ll bH \\ H/T & : T^{1+\alpha} \gg bH, \end{cases} \quad (41)$$

where b is a dimensionful non-universal constant. Similarly the entropy goes rapidly to zero at $T^{1+\alpha} \approx bH$ when the magnetic field starts to align the spins.

VI. COMMENTS ON THE RSRG SCHEME

In this section we discuss the validity of our RSRG treatment and various approximations we used. As we have seen in the previous sections, the formation of an effective spin yields new interactions among the remaining spins. These interactions were calculated perturbatively, where the (average) perturbation parameter is $\varepsilon = \Delta_t / \Delta_0$. To first order in ε , only nearest neighbor Heisenberg terms are induced, and the functional form of the Hamiltonian (1) is preserved in the RSRG transformation. However, the terms in (1) are not the only ones allowed by the symmetry, and in general we expect more complicated isotropic interactions to appear if higher order corrections in ε are included. In the original MDH RSRG, $\Delta_t / \Delta_0 \rightarrow 0$ as the fixed point is approached,¹⁷ and the perturbative treatment becomes exact. In our case ε stabilizes at a finite value around 0.2 at the fixed point. Thus we have to analyze here to what extent higher order terms can change our results.

The basic assumptions of the RSRG scheme are that the two spins which are most strongly coupled to each other form one effective spin, and that any breaking up of this spin pair involves such a large energy that we can regard the effective spin as a rigid object. There are two criteria for these assumptions to be valid. First, the energy cost for breaking up the strongest spin pair, i.e., the energy gap Δ , must be much larger than the energy available in neighboring spin pairs. Second, non-nearest neighbor couplings have to fall off sufficiently rapidly with distance, so that many weak couplings cannot accumulate sufficient strength to break up the spin pair. The second criterion is essentially equivalent to the absence of strong frustration in the system. Below, we argue that higher order terms do not lead to violation of any of these criteria, and hence that they do not qualitatively change any of our conclusions. In particular, the relations (16) between the scaling exponents, and hence the scaling forms (17) and (18), are still correct. The only impact higher order terms have, is to modify the expressions in Eq. (8) for the renormalized gaps, thereby slightly changing the average ratio a in Eq. (23) and the scaling exponent α . The low-temperature forms of the thermodynamic quantities derived in Sec. V are valid even though the actual value of the exponent α may shift slightly. In particular, it is important to note that the Curie-like form of the magnetic susceptibility does not involve α .

A. Higher order contributions

We consider effective interactions between spins which are separated by d (effective) lattice spacings. In the RG transformation these are generated by second (and higher) order terms in ε , and physically they represent interactions mediated by excitations within the locked effective spins. These terms will hence appear even if they are absent in the original Hamiltonian. However, the interactions generated in this way fall off exponentially with distance d as

$$\frac{\Delta(d)}{\Delta_0} \sim \varepsilon^d, \quad (42)$$

as can be seen from the following argument. For given energy scale Δ_0 , consider the strongest bond with spins S_L and S_R which are coupled via long-range interactions to the spins S_A and S_B , respectively, with the gaps $\Delta_{AL}/\Delta_0 \sim \varepsilon^{d_{AL}}$ and $\Delta_{RB}/\Delta_0 \sim \varepsilon^{d_{RB}}$ (see Fig. 7). The induced interaction between S_A and S_B due to second-order terms is

$$\frac{\Delta_{AB}}{\Delta_0} \sim \frac{\Delta_{AL}\Delta_{RB}}{\Delta_0^2} \sim \varepsilon^{d_{AL}+d_{RB}} . \quad (43)$$

Therefore the non-nearest neighbor interactions decay exponentially with $\varepsilon \approx 0.2$ at the fixed point and cannot lead to frustration effects. Consequently, it is justified to restrict our consideration to the dominating nearest-neighbor interactions only. The only remaining isotropic interactions are higher order nearest neighbor spin terms $(\mathbf{S}_i \cdot \mathbf{S}_{i+1})^m$. These terms are local and could in principle be included when calculating the lowest energy spin multiplet and the gap to the first excited state in a link. These higher power spin terms are also higher order in ε and are unlikely to become large enough to change the low-energy spectra of the strongest link qualitatively.

B. Three-spin decimation

For some particular combinations of spins and couplings, the renormalized gap becomes larger than the gap just removed, $\tilde{\Delta} > \Delta_0$.²³ In this section we argue that even in these cases it is justified to use the RG transformation outlined in Sec. II B.

For $\tilde{\Delta} > \Delta_0$ a more correct procedure would be to solve the three-spin problem involving the two spins on the strongest link and the spin on the link with $\tilde{\Delta} > \Delta_0$. We would represent the ground state multiplet of the three-spin system with one effective spin $\tilde{\mathbf{S}}$ and finally calculate the effective couplings between $\tilde{\mathbf{S}}$ and its neighbors (Fig. 9b). Here we claim that we can obtain essentially the same result using our RSRG scheme (Fig. 9a). In the first step the strongest link is replaced by an effective spin \mathbf{S}' , and the gaps Δ_1 and Δ_2 are renormalized. The renormalized gap $\tilde{\Delta}_2 > \Delta_0$ by assumption immediately becomes the largest gap in the chain so that, in the next step, the link $\{\tilde{\Delta}_2, S', S_2\}$ is replaced by an effective spin of size $\tilde{S} = |S' \pm S_2| = |S_L \pm S_R \pm S_2|$. In this process the gaps Δ_3 and Δ'_1 are renormalized. The size of the effective spin \tilde{S} in Fig. 9a is given by the absolute value of the (vector) sum of the spins \mathbf{S}_L , \mathbf{S}_R , and \mathbf{S}_2 parallel or antiparallel according to the sign of the couplings. This is the same spin we expect for the ground state multiplet of the three-spin system, i.e., $\tilde{\mathbf{S}}$ in Fig. 9b. Similarly we get the sign of the couplings between $\tilde{\mathbf{S}}$ and its neighbors in Fig. 9a from (8) by aligning the spins according to the signs of the couplings and by comparing the direction of the spins \mathbf{S}_1 and \mathbf{S}_3 with the direction of the effective spin $\tilde{\mathbf{S}}$. The signs of the couplings obtained in this way agree with what one expects for the signs of the corresponding couplings in the three-spin treatment in Fig. 9b. Therefore there can only be a difference in the renormalized coupling strengths between the twice-two-spin and three-spin decimation scheme. In both ways, however, the effective couplings $\tilde{\Delta}_1$ and $\tilde{\Delta}_3$ are proportional to Δ_1 and Δ_3 , respectively (and independent of the magnitude of the unphysically large gap $\tilde{\Delta}_2$ in the RG treatment). Therefore the discrepancy is minor and will not cause any qualitative difference.

VII. CONCLUSIONS AND SUMMARY

We have studied spin chains with random couplings and random spin sizes by means of a real-space RG scheme that successively replaces strongly correlated spin-pairs by effective spins. The RG transformation preserves the functional form of the Hamiltonian but changes the probability distribution of the links (couplings and spins). This procedure generates interactions among the remaining spins. For low enough energies the probability distribution of links acquire a scaling form, and for not too singular initial distributions of gaps (so that $\Delta^{y_c} P(\Delta)$ is regular, $y_c \approx 0.7$) the fixed-point distribution is universal. From a random walk picture for the formation of the large effective spins, we argue for a relation between the scaling exponents of length and the average spin size, which together with other considerations reduces the number of independent scaling exponents to one. This is confirmed in numerical simulations of random spin chains, and in the universal regime, we numerically determine the remaining independent scaling exponent to $\alpha = 0.22 \pm 0.01$.

At low energies (low temperatures) the random spin chain is characterized by large effective spins which interact weakly with their nearest neighbors. As temperature is further lowered, the average size of the effective spins increases as $T^{-\alpha}$ while the average distance between two effective spins (in units of the original lattice constant) increases as $T^{-2\alpha}$. This regime is also characterized by universal temperature dependence of thermodynamic quantities.

The slow approach to the fixed point (our numerical simulations indicate a crossover region of more than five orders of magnitude for reasonable starting configurations) suggests that the true scaling regime may be hard to reach in experiments. However, the formation of large effective spins occurs at considerably higher energy scale, and even if the scaling exponent α may not have stabilized to its fixed-point value, the distribution of links is roughly like the fixed-point distribution. The clearest signal of the formation of large effective spins is perhaps the Curie-like

temperature dependence of the uniform magnetic susceptibility, $\chi(T) \propto 1/T$, in a temperature regime $k_B T \leq J$ (J being the typical exchange interaction in the initial spin chain). Also, since the $1/T$ dependence in χ emerges before the distribution of links approaches the fixed point, the Curie-like susceptibility should be easier to address experimentally than other thermodynamic quantities which may develop scaling behavior only at inaccessibly low temperatures.

When the scaling regime is realized, the most straightforward way to measure the exponent α , and hence the rate at which spin degrees of freedom freeze out is through the specific heat, $C(T) \propto T^{2\alpha} |\ln T|$. An alternative approach which avoids the difficulties connected with measuring small heat transfers at low temperatures is to lower the temperature in the presence of a magnetic field until the magnetization saturates. The scaling exponent α may then be deduced from the predicted field dependence of the saturated magnetization, $M_{\text{sat}}(H) \propto H^{\frac{\alpha}{1+\alpha}}$.

The low-energy physics of the random spin chain studied in this paper is very different from that of uniform spin systems as well as spin- $\frac{1}{2}$ random bond antiferromagnetic chains studied in Refs. 14–17,19,20. In the RAF the ground state is a *random singlet phase* (RSP)²⁴ where each spin forms a singlet with another spin which may be located far away. In the RSP the coupling between two spins that have survived down to some energy scale Δ_0 is mediated by virtually exciting all intermediate singlets, leading to effective couplings that decreases exponentially with length, $J \propto \exp(-\sqrt{n})$. By inverting this relation it follows that length scales logarithmically with the energy, $n \propto |\ln \Delta_0|^2$. For the RSP, arguments analogous to those in Sec. V lead to entropy $\sigma(T, H = 0)/L \propto |\ln T|^{-2}$ and magnetic susceptibility $\chi(T)/L \propto T^{-1} |\ln T|^{-2}$.¹⁷ In our terminology this corresponds to $\alpha = \delta = 0$ up to logarithmic corrections. This is consistent with the interpretation of α in terms of the average renormalization factor a , Eq. (23). Indeed, in the case of the RAF the perturbative parameter $\varepsilon = \Delta_t/\Delta_0$ and hence also a goes to zero²⁵ near the fixed point, implying $\alpha = 0$. Clearly the RSP is distinct from the large-spin phase (LSP).

As pointed out in Ref. 19, a third possible state of random spin chains at low temperatures is the random dimer solid (RDS), which is easily understood within the MDH RG picture. Assuming that e.g., odd links are on average slightly stronger than even links in an antiferromagnetic spin- $\frac{1}{2}$ chain, the even links are correspondingly more likely to be removed. Since the removal of an even (odd) link leaves a renormalized odd (even) link behind, odd links are on average renormalized more frequently than even ones, and the separation in energy scale between even and odd links becomes more and more pronounced until all the singlets are on even links, the *random dimer solid*. Unlike the RSP and the LSP, thermodynamic quantities in the RDS show *non-universal* temperature dependence.¹⁹

The existence of various low-temperature fixed-points raises the question of stability of the various phases. As is expected from the discussion above, the RSP is unstable towards dimerization.¹⁹ In contrast, the large-spin fixed point is stable towards dimerization. Unlike the RSP in which spins are always removed in pairs, the RG transformation in general removes only one spin (i.e., replaces two spins with one effective spin). Hence odd links are turned into even ones and vice versa so that dimerization is irrelevant at the large-spin fixed point. From the discussion in Sec. III it is also clear that both the RSP and the RDS, which are singlet ground states, are unstable towards a small fraction of randomly distributed ferromagnetic bonds and/or large spins ($S > 1/2$). In both cases we expect the spin of the ground state to scale with length as $S^2 \sim L$ consistent with the fixed point studied in this paper. This has been confirmed in numerical simulations of random antiferromagnetic chains close to the random-singlet fixed point with 5% ferromagnetic bonds (chain E in Tab. I) or with 4% of the spins $S = 1$ (chain G). In all cases studied the chains first approach the fixed-point distribution of the RSP by forming singlets through the removal of $S = 1/2$ spins and AF links. However, as the density of higher spins and/or FM links increases, larger effective spins start to form and the distribution of links crosses over to the fixed-point distribution of the LSP. Which fixed point (either universal or non-universal) is eventually approached depends crucially on the initial distribution. This is because the singlet formation is very efficient in decreasing the effective couplings and quickly builds up a singular distribution of gaps. Hence, as long as only singlets are formed the distribution rapidly approaches the very singular random singlet fixed-point distribution. The degree of the singularity in the gap-distribution at the point where the density of $S \neq 1/2$ and ferromagnetic couplings becomes substantial, determines the behavior of the spin chain. If the singularity generated at this point is less than $P(\Delta) \sim \Delta^{-y_c}$ the chain will flow to the universal large-spin fixed point, while for stronger singularity the chain approaches one of the non-universal large-spin fixed points. This opens up an interesting possibility to access the non-universal fixed points in experiments by starting with a RAF with a properly chosen small fraction of FM bonds.

An interesting open question is what happens away from the Heisenberg point. Fisher extended the MDH RG to anisotropic antiferromagnetic spin- $\frac{1}{2}$ chains to show that also in the XY-regime ($J_i^z < J_i^x = J_i^y$) they flow to a random singlet fixed point, at least for broad enough initial distributions.¹⁷ The inclusion of anisotropy in the generalized MDH RG and its impact on the large-spin fixed point are interesting problems which we leave for future research.

ACKNOWLEDGMENTS

We would like to thank H.-C. zur Loya and T. N. Nguyen for stimulating our interest in the problem, and N. Nagaosa and T. K. Ng for helpful discussions. We are also grateful for the financial support by the Swedish Natural Science Research Council (E.W.), by Swiss Nationalfonds (M.S., No. 8220-037229), and by the MIT Science Partnership Fund. The work at MIT was supported primarily by the MRSEC Program of the National Science Foundation under Award Number DMR-9400334.

APPENDIX A: DERIVATION OF THE EFFECTIVE HAMILTONIAN

In this appendix we give a brief derivation of the effective couplings, Eqs. (7) and (9).

1. First-order perturbation theory

Consider the four-spin Hamiltonian

$$\mathcal{H} = \mathcal{H}_0 + \mathcal{H}_I \quad (\text{A1})$$

where

$$\mathcal{H}_0 = J_0 \mathbf{S}_L \cdot \mathbf{S}_R \quad (\text{A2a})$$

$$\mathcal{H}_I = J_1 \mathbf{S}_1 \cdot \mathbf{S}_L + J_2 \mathbf{S}_R \cdot \mathbf{S}_2 \quad (\text{A2b})$$

We treat \mathcal{H}_I as a perturbation to \mathcal{H}_0 . In the space of the degenerate ground states of \mathcal{H}_0 , the spins \mathbf{S}_L and \mathbf{S}_R form a state of maximum (minimum) total spin S for $J_0 < 0$ ($J_0 > 0$) while the spins \mathbf{S}_1 and \mathbf{S}_2 can point in any direction. The degenerate ground states span the Hilbert space \mathbf{H} , the product space of the spin spaces for \mathbf{S}_1 , \mathbf{S} and \mathbf{S}_2 . Each state $|m_1 M m_2\rangle = |m_1\rangle \otimes |M\rangle \otimes |m_2\rangle$ in \mathbf{H} is labeled by the corresponding azimuthal quantum numbers m_1 , M and m_2 . \mathcal{H}_I partly lifts the degeneracy and induces an effective Hamiltonian \mathcal{H}^{eff} in \mathbf{H} . To order $J_{1,2}/J_0$ the matrix elements of \mathcal{H}^{eff} are²⁶

$$\mathcal{H}_{m_1 M m_2, m'_1 M' m'_2}^{\text{eff}} = \langle m_1 M m_2 | \mathcal{H}_I | m'_1 M' m'_2 \rangle \quad (\text{A3})$$

We calculate \mathcal{H}^{eff} in two steps: We first establish the operator identities (valid in \mathbf{H})

$$\mathbf{S}_1 \cdot \mathbf{S}_L = c(S_L, S_R, S) \mathbf{S}_1 \cdot \mathbf{S} \quad (\text{A4a})$$

$$\mathbf{S}_2 \cdot \mathbf{S}_R = c(S_R, S_L, S) \mathbf{S}_2 \cdot \mathbf{S} \quad (\text{A4b})$$

which, together with Eqs. (A2b) and (A3), give

$$\mathcal{H}^{\text{eff}} = \tilde{J}_1 \mathbf{S}_1 \cdot \mathbf{S} + \tilde{J}_2 \mathbf{S} \cdot \mathbf{S}_2 \quad (\text{A5})$$

with

$$\tilde{J}_1 = J_1 c(S_L, S_R, S) \quad (\text{A6a})$$

$$\tilde{J}_2 = J_1 c(S_R, S_L, S) \quad (\text{A6b})$$

We then determine the constant $c(S_L, S_R, S)$ by calculating a suitable matrix element of the two operators in Eq. (A4a). To establish (A4a) we define the usual raising and lowering operators \hat{S}^\pm which act on a state $|M\rangle$ in a spin- S multiplet in the following way,

$$\begin{aligned} \hat{S}^- |M+1\rangle &= A_M^S |M\rangle \\ \hat{S}^+ |M\rangle &= A_M^S |M+1\rangle \end{aligned}$$

where the constants $A_M^S = \sqrt{(S-M)(S+M+1)}$ assure that $\langle M | M \rangle = 1$. Consider first the operators $\hat{S}_1^+ \hat{S}_L^-$ and $\hat{S}_1^+ \hat{S}_L^-$:

$$\langle m_1 M m_2 | \hat{S}_1^+ \hat{S}_- | m'_1 M' m'_2 \rangle = \delta_{m'_1, m_1-1} \delta_{M', M+1} \delta_{m'_2, m_2} A_{m_1-1}^{S_1} A_M^S \quad (A7a)$$

$$\langle m_1 M m_2 | \hat{S}_1^+ \hat{S}_L^- | m'_1 M' m'_2 \rangle = \delta_{m'_1, m_1-1} \delta_{M', M+1} \delta_{m'_2, m_2} A_{m_1-1}^{S_1} \langle M | \hat{S}_L^- | M+1 \rangle \quad (A7b)$$

The matrix element in the right hand side of Eq. (A7b) is

$$\begin{aligned} \langle M | \hat{S}_L^- | M+1 \rangle &= (A_{M+1}^S A_{M+2}^S \cdots A_{S-1}^S)^{-1} \langle M | \hat{S}_L^- (\hat{S}^-)^{S-M-1} | S \rangle \\ &= A_M^S (A_{S-1}^S)^{-1} \langle S-1 | \hat{S}_L^- | S \rangle \quad , \end{aligned} \quad (A8)$$

where we have used the fact that $\hat{S}^- = \hat{S}_L^- + \hat{S}_R^-$ commutes with \hat{S}_L^- . From Eqs. (A7a), (A7b) and (A8) we see that

$$\hat{S}_1^+ \hat{S}_L^- = (A_{S-1}^S)^{-1} \langle S-1 | \hat{S}_L^- | S \rangle \hat{S}_1^+ \hat{S}^- \quad (A9)$$

for every combination of $m_1 \dots M'$, i.e., as an operator identity in \mathbf{H} . We note that $\langle S-1 | \hat{S}_L^- | S \rangle$ is a real number, and take conjugation of Eq. (A9):

$$\hat{S}_1^- \hat{S}_L^+ = (A_{S-1}^S)^{-1} \langle S-1 | \hat{S}_L^- | S \rangle \hat{S}_1^- \hat{S}^+.$$

We obtain the operator identity

$$\hat{S}_1^x \hat{S}_L^x + \hat{S}_1^y \hat{S}_L^y = (A_{S-1}^S)^{-1} \langle S-1 | \hat{S}_L^- | S \rangle \left(\hat{S}_1^x \hat{S}^x + \hat{S}_1^y \hat{S}^y \right) \quad . \quad (A10)$$

Equation (A4a) then follows from Eq. (A10) and rotational invariance. From the relation $\langle S-1 | \hat{S}_L^- | S \rangle = (A_{S-1}^S)^{-1} \langle S | \hat{S}^+ \hat{S}_L^- | S \rangle = 2(A_{S-1}^S)^{-1} \langle S | \hat{S}_L^z | S \rangle$ we obtain

$$c(S_L, S_R, S) = \frac{\langle S | \hat{S}_L^z | S \rangle}{S} \quad . \quad (A11)$$

To determine $\langle S | \hat{S}_L^z | S \rangle$ in Eq. (A11) we evaluate the matrix element $\langle S | \mathbf{S}_L \cdot \mathbf{S} | S \rangle$ in two different ways. First we use $\mathbf{S} = \mathbf{S}_L + \mathbf{S}_R$ to get

$$\begin{aligned} \langle S | \mathbf{S}_L \cdot \mathbf{S} | S \rangle &= \langle S | \mathbf{S}_L^2 | S \rangle + \langle S | \mathbf{S}_L \cdot \mathbf{S}_R | S \rangle \\ &= \frac{1}{2} [S(S+1) + S_L(S_L+1) - S_R(S_R+1)] \quad . \end{aligned} \quad (A12)$$

The same matrix element can also be written as

$$\langle S | \mathbf{S}_L \cdot \mathbf{S} | S \rangle = \langle S | \hat{S}_L^z \hat{S}^z | S \rangle + \frac{1}{2} \langle S | \hat{S}_L^- \hat{S}^+ | S \rangle + \frac{1}{2} \langle S | \hat{S}_L^+ \hat{S}^- | S \rangle \quad . \quad (A13)$$

The first term in Eq. (A13) equals $S \langle S | \hat{S}_L^z | S \rangle$, the second term vanishes since $|S\rangle$ is a highest weight state, and for the same reason we can replace the operator $\hat{S}_L^+ \hat{S}^-$ in the third term by the commutator $[\hat{S}_L^+, \hat{S}^-] = 2\hat{S}_L^z$ so that

$$\langle S | \mathbf{S}_L \cdot \mathbf{S} | S \rangle = (S+1) \langle S | \hat{S}_L^z | S \rangle \quad . \quad (A14)$$

From Eqs. (A12), (A14), and (A11) finally follows

$$c(S_L, S_R, S) = \frac{S(S+1) + S_L(S_L+1) - S_R(S_R+1)}{2S(S+1)} \quad . \quad (A15)$$

For the three cases of interest to us, Eqs. (A15) and (A6) give

$$\tilde{J}_1 = \begin{cases} J_1 \frac{S_L}{S_L + S_R} & : J_0 < 0 \\ J_1 \frac{S_L + 1}{S_L - S_R + 1} & : J_0 > 0, S_L > S_R \\ -J_1 \frac{S_L}{S_R - S_L + 1} & : J_0 > 0, S_L < S_R \end{cases} \quad (A16)$$

and

$$\tilde{J}_2 = \begin{cases} J_2 \frac{S_R}{S_L + S_R} & : J_0 < 0 \\ -J_2 \frac{S_R}{S_L - S_R + 1} & : J_0 > 0, S_L > S_R \\ J_2 \frac{S_R + 1}{S_R - S_L + 1} & : J_0 > 0, S_L < S_R \end{cases} \quad (A17)$$

from which Eqs. (8) follow by using the relation between couplings J and gaps Δ , Eqs. (5).

2. The effective coupling in the case of singlet formation: generalization of the MDH RG transformation

In the case where $J_0 > 0$ and $S_L = S_R$, the effective spin is a singlet, $S = 0$, and the effective Hamiltonian, Eq. (A3), vanishes. To get a nonzero coupling between S_1 and S_2 , we have to include second order perturbation. In the case $S_L = S_R = \frac{1}{2}$ this gives the effective couplings used in the MDH RG. Since the first order contribution is zero, we have to solve the second-order secular equation²⁶

$$\text{Det} \left(V_{gg'} - E^{(2)} \delta_{gg'} \right) = 0 \quad (\text{A18})$$

with

$$V_{gg'} = \sum_e \frac{\langle g | \mathcal{H}_I | e \rangle \langle e | \mathcal{H}_I | g \rangle}{E_0 - E_e} , \quad (\text{A19})$$

where $|g\rangle$ is a ground state of \mathcal{H}_0 , the sum is over all excited states $|e\rangle$ and E_e is the (unperturbed) energy of the state $|e\rangle$. Since there is no coupling between the outer spins if either J_1 or J_2 is zero, only terms proportional to $J_1 J_2$ in Eq. (A19) contribute to the effective coupling (the terms proportional to J_1^2 and J_2^2 give an overall energy shift which, for our purposes, can be discarded). Denoting the states formed by the spins S_1 and S_2 by $|A\rangle$, the states formed by S_R and S_L by $|B\rangle$ and in particular the ground state singlet by $|B = 0\rangle$ we have (in obvious notation)

$$\begin{aligned} V_{AA} = & 2J_1 J_2 \sum_{A', B'} \frac{\langle A, 0 | \hat{S}_1^z \hat{S}_L^z | A', B' \rangle \langle A', B' | \hat{S}_R^z \hat{S}_2^z | A, 0 \rangle}{-J_0 \frac{1}{2} S_{B'} (S_{B'} + 1)} \\ & + \frac{J_1 J_2}{2} \sum_{A', B'} \frac{\langle A, 0 | \hat{S}_1^- \hat{S}_L^+ | A', B' \rangle \langle A', B' | \hat{S}_R^- \hat{S}_2^+ | A, 0 \rangle}{-J_0 \frac{1}{2} S_{B'} (S_{B'} + 1)} \\ & + \frac{J_1 J_2}{2} \sum_{A', B'} \frac{\langle A, 0 | \hat{S}_1^+ \hat{S}_L^- | A', B' \rangle \langle A', B' | \hat{S}_R^+ \hat{S}_2^- | A, 0 \rangle}{-J_0 \frac{1}{2} S_{B'} (S_{B'} + 1)} . \end{aligned} \quad (\text{A20})$$

The sum over the states $|A'\rangle$ can be performed separately to give

$$\begin{aligned} V_{AA} = & -\frac{4J_1 J_2}{J_0} \langle A | \hat{S}_1^z \hat{S}_2^z | A \rangle \sum_{B'} \frac{\langle 0 | \hat{S}_L^z | B' \rangle \langle B' | \hat{S}_R^z | 0 \rangle}{S_{B'} (S_{B'} + 1)} \\ & -\frac{J_1 J_2}{J_0} \langle A | \hat{S}_1^+ \hat{S}_2^- | A \rangle \sum_{B'} \frac{\langle 0 | \hat{S}_L^- | B' \rangle \langle B' | \hat{S}_R^+ | 0 \rangle}{S_{B'} (S_{B'} + 1)} \\ & -\frac{J_1 J_2}{J_0} \langle A | \hat{S}_1^- \hat{S}_2^+ | A \rangle \sum_{B'} \frac{\langle 0 | \hat{S}_L^+ | B' \rangle \langle B' | \hat{S}_R^- | 0 \rangle}{S_{B'} (S_{B'} + 1)} . \end{aligned} \quad (\text{A21})$$

The matrix elements in the sums get contributions only from spin-1 multiplets, and hence we can extract the factor $1/[S_{B'} (S_{B'} + 1)] = 1/2$ and perform the sum over the complete set of states $|B'\rangle$. Finally, since

$$\langle 0 | \hat{S}_L^z \hat{S}_R^z | 0 \rangle = \frac{1}{2} \langle 0 | \hat{S}_L^+ \hat{S}_R^- | 0 \rangle = \frac{1}{2} \langle 0 | \hat{S}_L^- \hat{S}_R^+ | 0 \rangle = \frac{1}{3} \langle 0 | \mathbf{S}_L \cdot \mathbf{S}_R | 0 \rangle = -\frac{1}{3} S_L (S_L + 1) \quad (\text{A22})$$

we have

$$V_{AA} = \frac{2J_1 J_2 S_L (S_L + 1)}{3J_0} \langle A | \mathbf{S}_1 \cdot \mathbf{S}_2 | A \rangle \quad (\text{A23})$$

from which it is clear that the effective Hamiltonian in this case is

$$\mathcal{H}^{\text{eff}} = \tilde{J} \mathbf{S}_1 \cdot \mathbf{S}_2 \quad (\text{A24})$$

with

$$\tilde{J} = \frac{2J_1 J_2 S_L (S_L + 1)}{3J_0} . \quad (\text{A25})$$

In the special case of $S_L = S_R = 1/2$ this gives $\tilde{J} = J_1 J_2 / 2J_0$ in agreement with Ref. 14.

APPENDIX B: THE GENERALIZATION OF THE MDH RG FLOW EQUATIONS

Although in this paper we have studied the RG flow by numerical simulations, it is of interest to show that flow equations of the form Eqs. (13) exist and can be expected to have attractive fixed point(s) to which the probability distributions eventually flow. Rather than deriving the explicit forms of F_1 and F_2 , which are rather complicated, we will outline how this can be done and point out to what extent the generalized flow equations (13) differ from the MDH RG flow equation (4).

We may view one step in the RG transformation as the removal of one link $\{\Delta_0, S_L, S_R\}$ and the change of two links, $\{\Delta_1, S_1, S_L\}, \{\Delta_2, S_R, S_2\} \rightarrow \{\tilde{\Delta}_1, S_1, S\}, \{\tilde{\Delta}_2, S, S_2\}$. For an infinitely long chain we remove a small fraction of links with gaps in the interval $[\Delta_0 - d\Delta_0, \Delta_0]$. This is illustrated in Fig. 10, where, for convenience, we show $P^A(\Delta_0; \Delta, S_L, S_R)$ and $P^F(\Delta_0; -\Delta, S_L, S_R)$ in the same diagram. At an energy scale Δ_0 , P^A and P^F are non-zero only for links with $\Delta \leq \Delta_0$. We remove all links in the thin shell $\Delta \in [\Delta_0 - d\Delta_0, \Delta_0]$, which causes a small fraction of links inside the equal-gap surface $\Delta = \Delta_0$ to hop around. The changes in P^A and P^F due to the links that move around are of order $d\Delta_0$ so that in the limit $d\Delta_0 \rightarrow 0$ the RG flow is described by a set of first-order differential equations

$$\frac{dP^A}{d\Delta_0} = F_1[P^A, P^F], \quad (B1a)$$

$$\frac{dP^F}{d\Delta_0} = F_2[P^A, P^F], \quad (B1b)$$

where F_1 and F_2 are two (non-linear) functionals of P^A and P^F , whose explicit forms depend on the functions f_n in Eq. (8). If renormalized gaps were always smaller than Δ_0 , it would be straightforward to write down the explicit form of the flow equations (13). Assuming no correlations between neighboring links (except for the obvious correlation that they share one spin), we find four types of terms in F_1 ; (i) One term proportional to $-\delta(\Delta - \Delta_0)P^A$ that depletes the region of links where $\Delta \in [\Delta_0 - d\Delta_0, \Delta_0]$. (ii) One term that decreases P^A due to links $\{\Delta, S_1, S_L\}$ that are transformed because they neighbor a link that is replaced by an effective spin. (iii) A set of terms that increase $P^A(\Delta_0; \tilde{\Delta}_1, S_1, S)$ because some links are transformed into links $\{\tilde{\Delta}_1, S_1, S\}$. (iv) One term proportional to P^A that compensates for the overall decrease in the number of links and keeps the probability distributions normalized. The functional F_2 has a similar structure. Only the third kind of terms involve the RG functions f_n . We note that in the original MDH RG the terms (ii) and (iv) cancel. The term (i) can be omitted if the probability distribution is defined only on the interval $[0, \Delta_0]$. This was done in Ref. 14 so that the only term that appears in Eq. (4) is one term of type (iii).

If some renormalized gaps become larger than Δ_0 , then before we take the limit $d\Delta_0 \rightarrow 0$ we must consider the fraction of the transformed links that acquire $\tilde{\Delta} > \Delta_0$. As we have discussed in Sec. VIB, in our RG scheme a finite fraction of the links acquires a larger gap $\tilde{\Delta} > \Delta_0$; in Fig. 10 this corresponds to links that jump outside the support of P^A and P^F . If the unphysically strong links are not taken care of before the next slice of links are removed, more and more links will end up outside the Δ_0 surface. In the limit $d\Delta_0 \rightarrow 0$ this will make it impossible to define Δ_0 , since smoothly integrating out links in a finite gap interval in this case generates a small but finite probability for gaps of *any* strength. This problem is remedied in the following way. Since in our RG scheme, no property of the renormalized links depends on the actual value of the gap in the strongest link, we can modify the equations (7) so that $\tilde{\Delta} = \min\{\Delta f_n, \Delta_0\}$. This does not change the discrete RG scheme since the renormalized link is removed in the next step of the RG after which there is no information in the chain of the value of $\tilde{\Delta}$. In Fig. 10, this modification of the functions f_n is illustrated by projecting strong links back onto the surface $\Delta = \Delta_0$. The projected links are then removed, which transforms some links in P^A and P^F , and also generates an even smaller fraction of links above the Δ_0 -surface. These links are then projected and removed etc. Keeping terms of order $d\Delta_0$, the infinite sequence of removing smaller and smaller fractions of links that in the previous step have jumped out of the distribution contributes a series of smaller and smaller terms in the shift of P^A and P^F that has to be summed before the limit $d\Delta_0 \rightarrow 0$ is taken. This resummation makes the functionals $F_{1,2}$ in (13) rather complicated.

* Present address: Department of Theoretical Physics, Royal Institute of Technology, S-10044 Stockholm, Sweden.

† Present address: Yukawa Institute for Theoretical Physics, Kyoto University, Kyoto 606-01, Japan.

[‡] Present address: Theoretische Physik, ETH-Hönggerberg, 8093 Zürich, Switzerland.

¹ See, e.g., E. Fradkin, *Field Theories of Condensed Matter Systems*, (Addison-Wesley, Redwood City, CA, 1991).

² M. den Nijs and K. Rommelse, Phys. Rev. B **40**, 4709 (1989); K. Hida, *ibid.* **45**, 2207 (1992).

³ F. D. M. Haldane, Phys. Rev. Lett. **67**, 937 (1991).

⁴ J. P. Renard *et al.*, J. Appl. Phys. **63**, 3538 (1988); M. Date and K. Kindo, Phys. Rev. Lett. **65**, 1659 (1990).

⁵ J. S. Miller (editor), *Extended Linear Chain Compounds*, Vol. 3, (Plenum Press, New York, 1983).

⁶ A. P. Wilkinson, and A. K. Cheetham, Acta Cryst. C **45**, 1672 (1989); A. P. Wilkinson, A. K. Cheetham, W. Kunnman, and A. Kvick, Eur. J. Solid State Inorg. Chem. **28** 453 (1991).

⁷ J. J. Randall, and L. Katz, Acta Cryst. **12**, 519 (1959).

⁸ C. A. Doty and D. S. Fisher, Phys. Rev. B **45**, 2167 (1992); see also K. J. Runge and G. T. Zimanyi, *ibid.* **49**, 15212 (1994) and references therein.

⁹ L. N. Bulaevskii, A. V. Zvarykina, Y. S. Karimov, R. B. Lyubovskii and I. F. Shchegolev, Zh. Eksp. Teor. Fiz. **62**, 725 (1972) [Sov. Phys. JETP **35**, 384 (1972)].

¹⁰ T. N. Nguyen, Ph. D. thesis, Massachusetts Institute of Technology, (1994) (unpublished); T. N. Nguyen, D. M. Giaquinta, and H.-C. zur Loya, Chem. Mater. **6**, 1642, (1994), T. N. Nguyen and H.-C. zur Loya, J. Solid State Chem. **117**, 300 (1995).

¹¹ A. Furusaki, M. Sigrist, P. A. Lee, K. Tanaka, and N. Nagaosa, Phys. Rev. Lett. **73**, 2622 (1994); T. N. Nguyen, P. A. Lee, and H.-C. zur Loya, Science **271**, 489 (1996).

¹² A. Furusaki, M. Sigrist, E. Westerberg, P. A. Lee, K. B. Tanaka, and N. Nagaosa, Phys. Rev. B **52**, 15930 (1995).

¹³ Another system whose low-energy physics is described by Eq. (1) is the randomly depleted Heisenberg ladder, see M. Sigrist and A. Furusaki, J. Phys. Soc. Jpn. **65**, 2385 (1996).

¹⁴ S.-k. Ma, C. Dasgupta, and C.-k. Hu, Phys. Rev. Lett. **43**, 1434 (1979); C. Dasgupta and S.-k. Ma, Phys. Rev. B **22**, 1305 (1980).

¹⁵ J. E. Hirsch and J. V. José, Phys. Rev. B **22**, 5339 (1980); J. E. Hirsch, *ibid.* **22**, 5355 (1980).

¹⁶ K. Hida, J. Phys. Soc. Jpn. **65**, 895 (1996).

¹⁷ D. S. Fisher, Phys. Rev. B **50**, 3799 (1994).

¹⁸ E. Westerberg, A. Furusaki, M. Sigrist, and P. A. Lee, Phys. Rev. Lett. **75**, 4302 (1995), see also Ref. 12.

¹⁹ R. A. Hyman, Kun Yang, R. N. Bhatt, and S. M. Girvin, Phys. Rev. Lett. **76**, 839 (1996).

²⁰ R. A. Hyman, Ph. D. thesis, Indiana University (1996) (unpublished).

²¹ Exceptions to this are spin chains with different bond distribution on even and odd links which eventually flow to a random dimer solid. This is not in contradiction with the results in Ref. 17 since in these systems two neighboring bonds are not uncorrelated and Eq. (4) is no longer valid *c.f.* Ref. 19.

²² As pointed out by Hyman in his thesis,²⁰ this is not the only choice for the characteristic energy scale under which one can regard two spins as a single object. In fact, he suggested to take $\Delta = |J|S_2(2S_1 + 1)$ for $S_1 > S_2$, which is the gap between the ground state and highest energy state.

²³ For example, let the strongest link be antiferromagnetic while the neighboring links are ferromagnetic and set $S_1 = 10$, $S_L = 2$, $S_R = 1$. Then $\tilde{\Delta}_1$ will be larger than Δ_0 if $\Delta_1 > \frac{8}{11}\Delta_0$.

²⁴ R. N. Bhatt and P. A. Lee, Phys. Rev. Lett. **48**, 344 (1982).

²⁵ We point out that in the random singlet phase, $\beta \neq 1$ is allowed because the fixed-point distribution is strictly speaking not normalizable.

²⁶ See, e.g., L. D. Landau and E. M. Lifshitz, *Quantum Mechanics (non-relativistic theory)*, chapter VI, (Pergamon Press, Oxford, 1977).

Chain	$P_F(\Delta)$	$P_A(\Delta)$	$Q(S)$	$x = N_A/N$	length
A	$1 - \Delta$	$1 - \Delta$	$\frac{1}{20} \sum_{n=1}^{20} \delta(S - \frac{n}{2})$	50%	10^6
B	Δ	Δ	$\frac{1}{4} \sum_{g=1}^4 \delta(S - \frac{g}{2})$	50%	10^6
C	0	1	$\frac{1}{8} \sum_{n=1}^8 \delta(S - \frac{n}{2})$	100%	10^6
D	0.75	0.25	$\frac{1}{4} \sum_{n=1}^4 \delta(S - \frac{n}{2})$	25%	$5 \cdot 10^5$
E	0.05	$0.2375 \cdot \Delta^{-3/4}$	$\delta(S - \frac{1}{2})$	95%	10^6
F	$\frac{1}{2} \Delta^{-1/2}$	$\frac{1}{2} \Delta^{-1/2}$	$\frac{1}{4} \sum_{n=1}^4 \delta(S - \frac{n}{2})$	50%	10^5
G	0	$\frac{1}{4} \Delta^{-3/4}$	$0.96 \delta(S - \frac{1}{2}) + 0.04 \delta(S - 1)$	100%	10^6
H	$\frac{2}{5} \Delta^{-3/5}$	$\frac{2}{5} \Delta^{-3/5}$	$\frac{1}{4} \sum_{n=1}^4 \delta(S - \frac{n}{2})$	50%	10^5
I	$\frac{1}{3} \Delta^{-2/3}$	$\frac{1}{3} \Delta^{-2/3}$	$\frac{1}{4} \sum_{n=1}^4 \delta(S - \frac{n}{2})$	50%	10^5
J	$\frac{2}{7} \Delta^{-5/7}$	$\frac{2}{7} \Delta^{-5/7}$	$\frac{1}{4} \sum_{n=1}^4 \delta(S - \frac{n}{2})$	50%	10^5
K	$\frac{1}{4} \Delta^{-3/4}$	$\frac{1}{4} \Delta^{-3/4}$	$\frac{1}{4} \sum_{n=1}^4 \delta(S - \frac{n}{2})$	50%	$1.2 \cdot 10^6$
L	$\frac{2}{9} \Delta^{-7/9}$	$\frac{2}{9} \Delta^{-7/9}$	$\frac{1}{4} \sum_{n=1}^4 \delta(S - \frac{n}{2})$	50%	10^5
M	$\frac{1}{5} \Delta^{-4/5}$	$\frac{1}{5} \Delta^{-4/5}$	$\frac{1}{4} \sum_{n=1}^4 \delta(S - \frac{n}{2})$	50%	10^5
N	$\frac{2}{11} \Delta^{-9/11}$	$\frac{2}{11} \Delta^{-9/11}$	$\frac{1}{4} \sum_{n=1}^4 \delta(S - \frac{n}{2})$	50%	10^5
O	$\frac{1}{8} \Delta^{-7/8}$	$\frac{1}{8} \Delta^{-7/8}$	$\frac{1}{4} \sum_{n=1}^4 \delta(S - \frac{n}{2})$	50%	10^6
P	$\frac{1}{6} \Delta^{-5/6}$	$\frac{1}{6} \Delta^{-5/6}$	$\frac{1}{4} \sum_{n=1}^4 \delta(S - \frac{n}{2})$	50%	10^5

TABLE I. The initial conditions for the 16 chains simulated numerically.

FIG. 1. Schematic pictures of the RG scheme. (a) The original MDH decimation. (b) Definition of a link as two neighboring spins S_L and S_R and the gap Δ . (c) The generalized MDH decimation.

FIG. 2. (a) The antiferromagnetic fixed-point distribution of spins and gaps, $Q_{S\Delta}^A(\Delta/\Delta_0, S) = \int_0^\infty dS' Q^A(\Delta/\Delta_0, S, S')$. The spins are in units of $\langle S \rangle$ and the distribution is normalized according to (11). (b) The ferromagnetic fixed-point distribution of spins and gaps, $Q_{S\Delta}^F(\Delta/\Delta_0, S)$, defined analogously to $Q_{S\Delta}^A$ in (a). (c) The antiferromagnetic fixed-point distributions of left and right spins, $Q_{SS}^A(S, S') = \int_0^1 dx Q^A(x, S, S')$. The units and normalization are as in (a). (d) The ferromagnetic fixed-point distributions of left and right spins, $Q_{SS}^F(S, S')$, defined analogously to Q_{SS}^A in (c) and with units and normalization as in (a).

FIG. 3. (a) The distributions of gaps at the fixed point, $Q_{\Delta}^{A,F}(\Delta/\Delta_0) = \int_0^\infty dS dS' Q^{A,F}(\Delta/\Delta_0, S, S')$. (b) The distributions of spins at the fixed point, $Q_S^{A,F}(S) = \int_0^1 dx \int_0^\infty dS' Q^{A,F}(x, S, S')$. The spins are in units of $\langle S \rangle$.

FIG. 4. (a) The average gap $\langle \Delta \rangle$ as a function of Δ_0 in chain C in Tab. I. (b) The average spin $\langle S \rangle$ and length n as a function of Δ_0 in chain C in Tab. I.

FIG. 5. Effective exponents as functions of Δ_0^{-1} in chain C in Tab. I.

FIG. 6. The fixed-point distributions of AF gaps for four singular chains (chains E, G, K and O in Tab. I) (dotted lines). These are to be compared with the corresponding fixed-point distribution of regular chains (solid line)

FIG. 7. Log-log plot of the distribution of gaps at the fixed point for regular initial distributions.

FIG. 8. Higher order terms induce a coupling between S_A and S_B as S_L and S_R are replaced by an effective spin.

FIG. 9. (a) The two-step decimation of three spins used in the numerical simulations. (b) The three-spin decimation in one step.

FIG. 10. The link distributions are non-zero only for $\Delta < \Delta_0$. Replacing gaps in the thin slice $\Delta \in [\Delta_0 - d\Delta_0, \Delta_0]$ shifts a fraction of links in P^A and P^F .

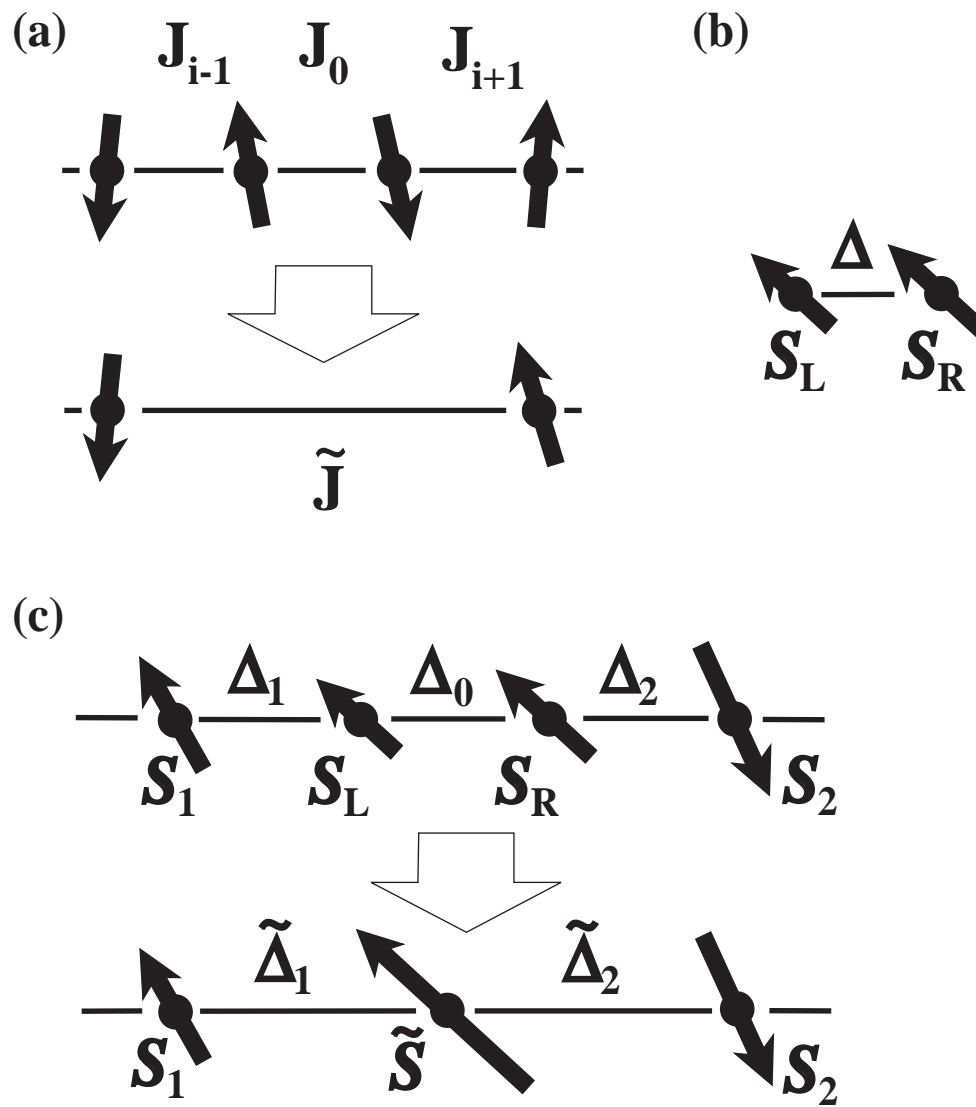


Figure 2a in the article "The low-energy fixed points of random quantum spin chains" by E. Westerberg, A. Furusaki, M. Sigrist, and P. A. Lee.

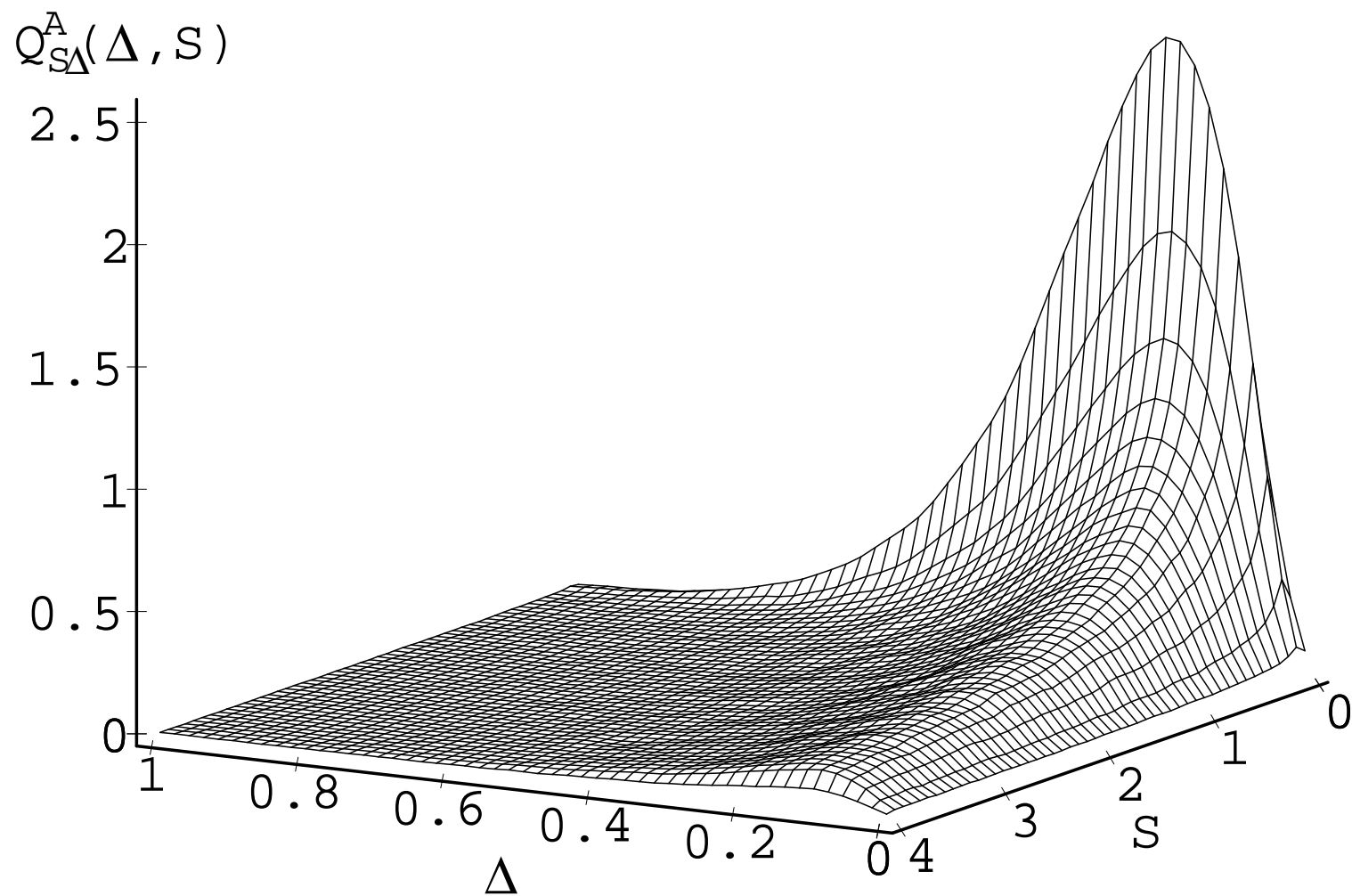


Figure 2b in the article "The low-energy fixed points of random quantum spin chains" by E. Westerberg, A. Furusaki, M. Sigrist, and P. A. Lee.

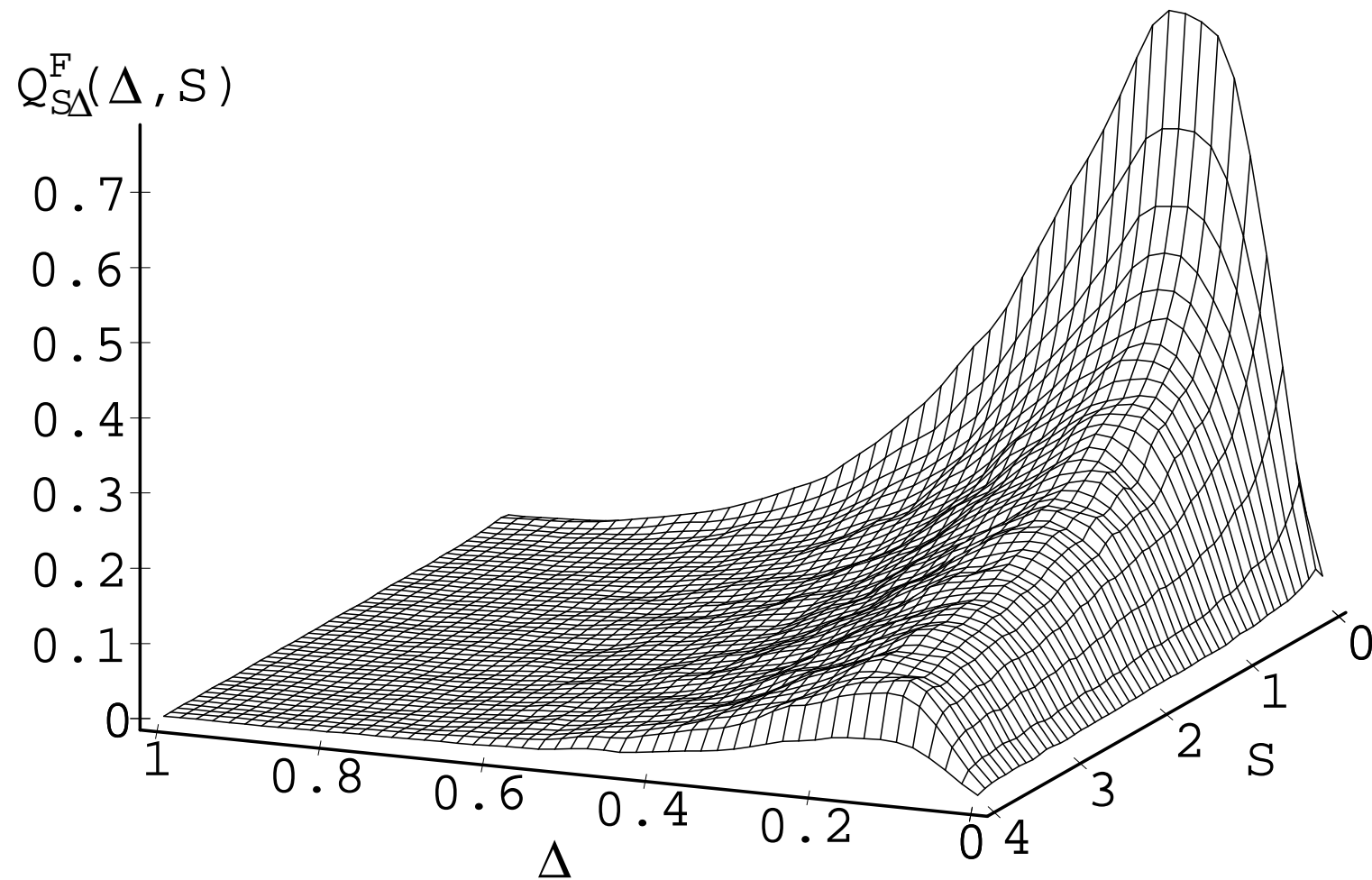


Figure 2c in the article "The low-energy fixed points of random quantum spin chains" by E. Westerberg, A. Furusaki, M. Sigrist, and P. A. Lee.

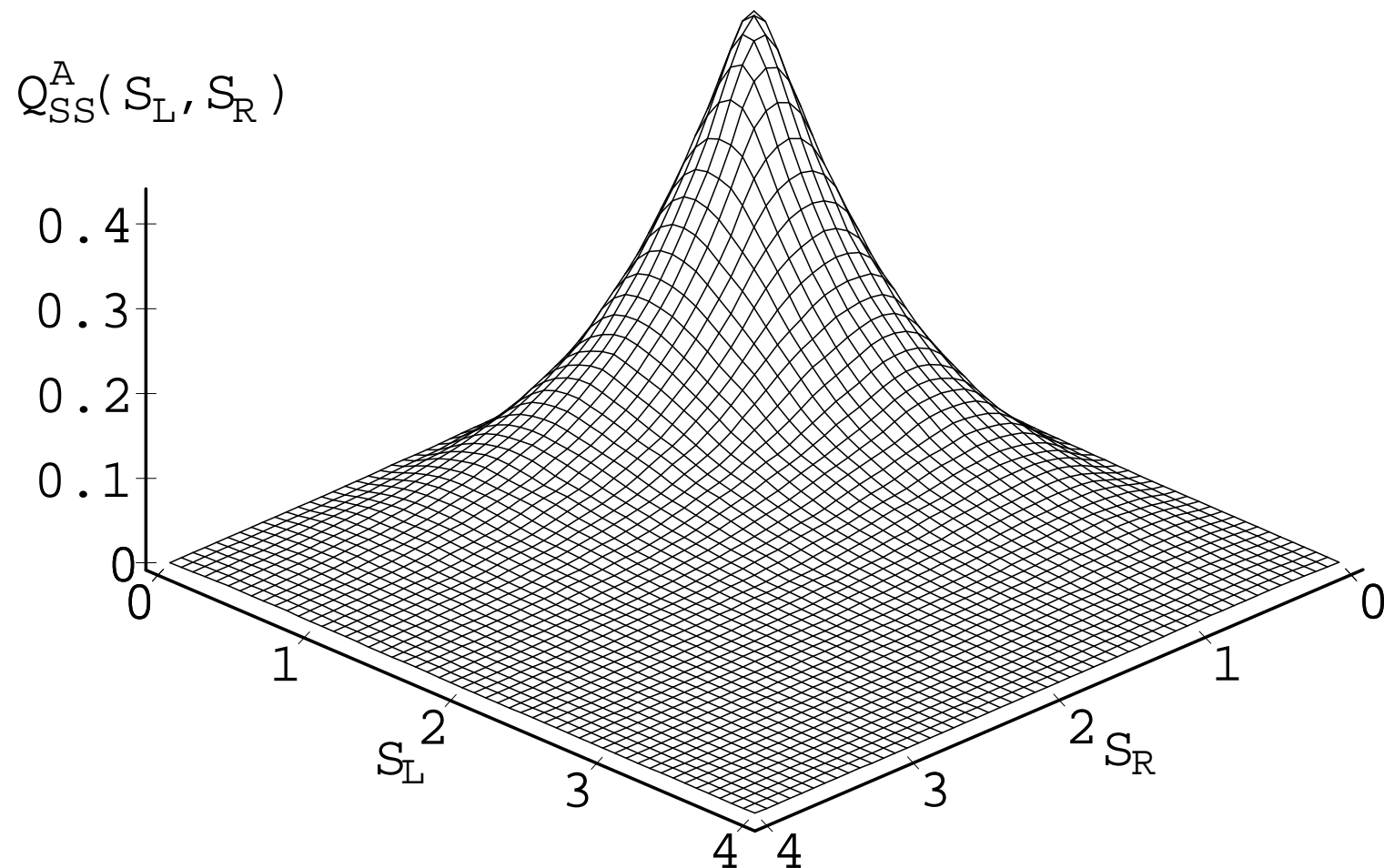


Figure 2d in the article "The low-energy fixed points of random quantum spin chains" by E. Westerberg, A. Furusaki, M. Sigrist, and P. A. Lee.

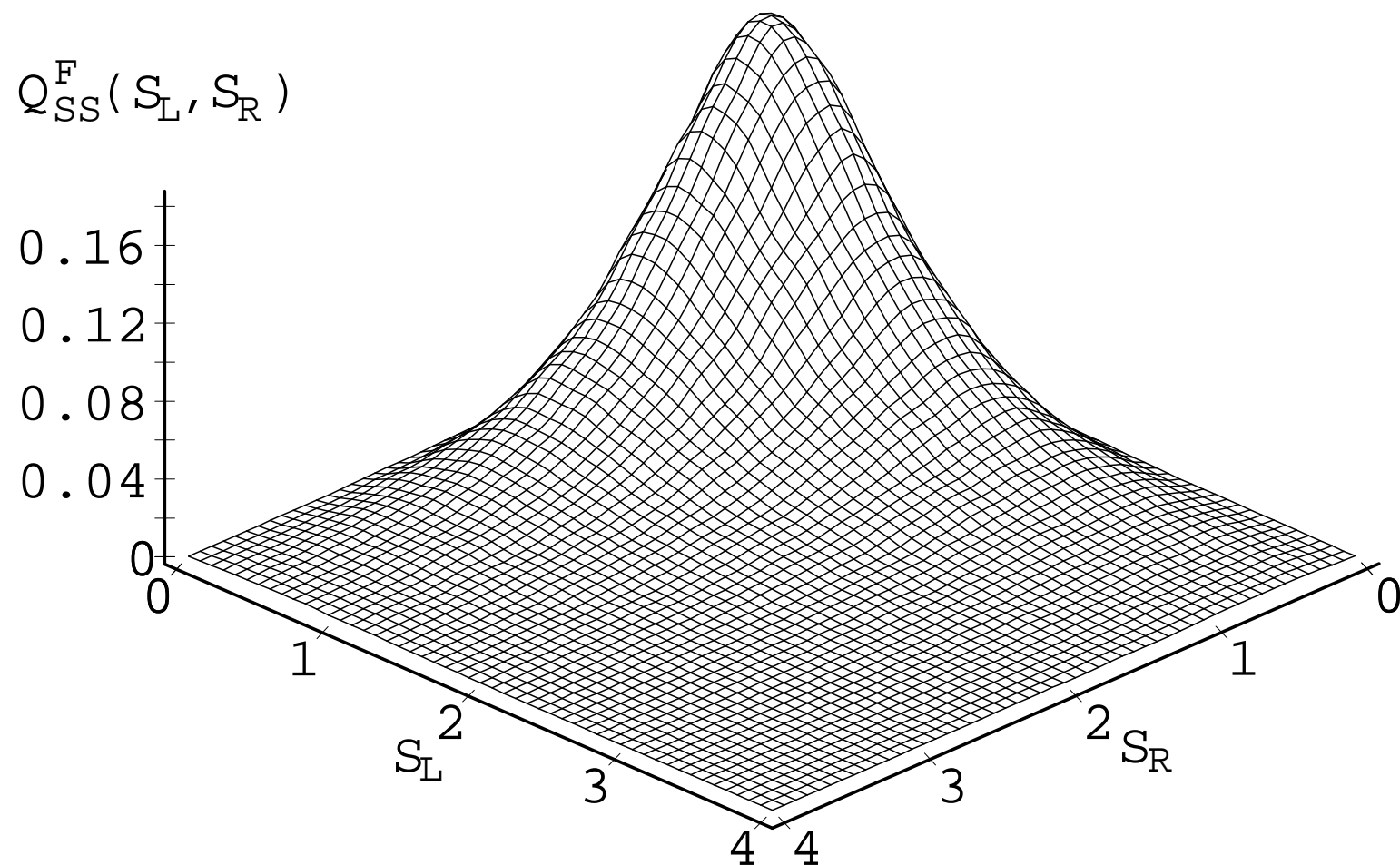


Figure 3 in the article "The low-energy fixed points of random quantum spin chains" by E. Westerberg, A. Furusaki, M. Sigrist, and P. A. Lee.

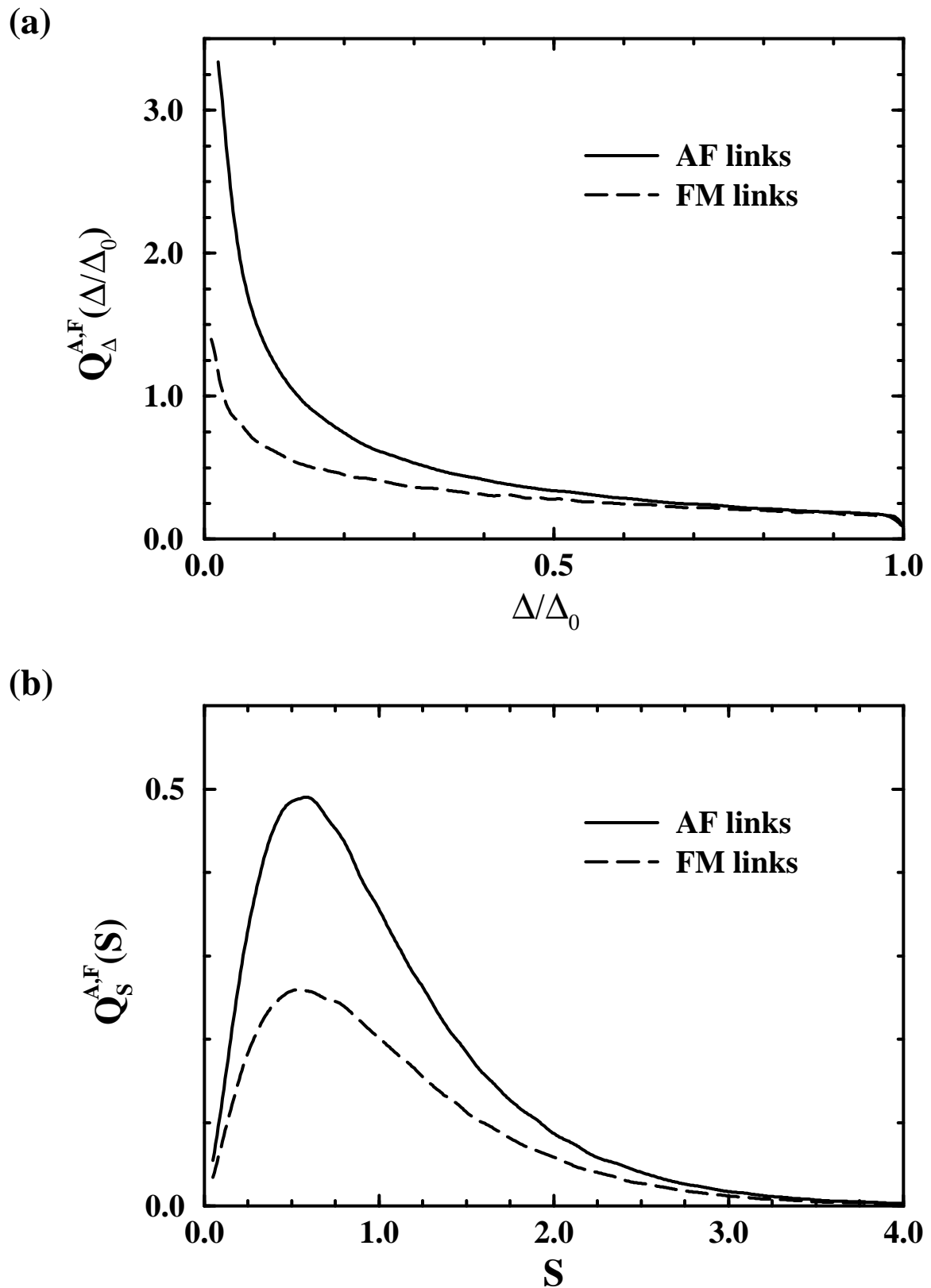
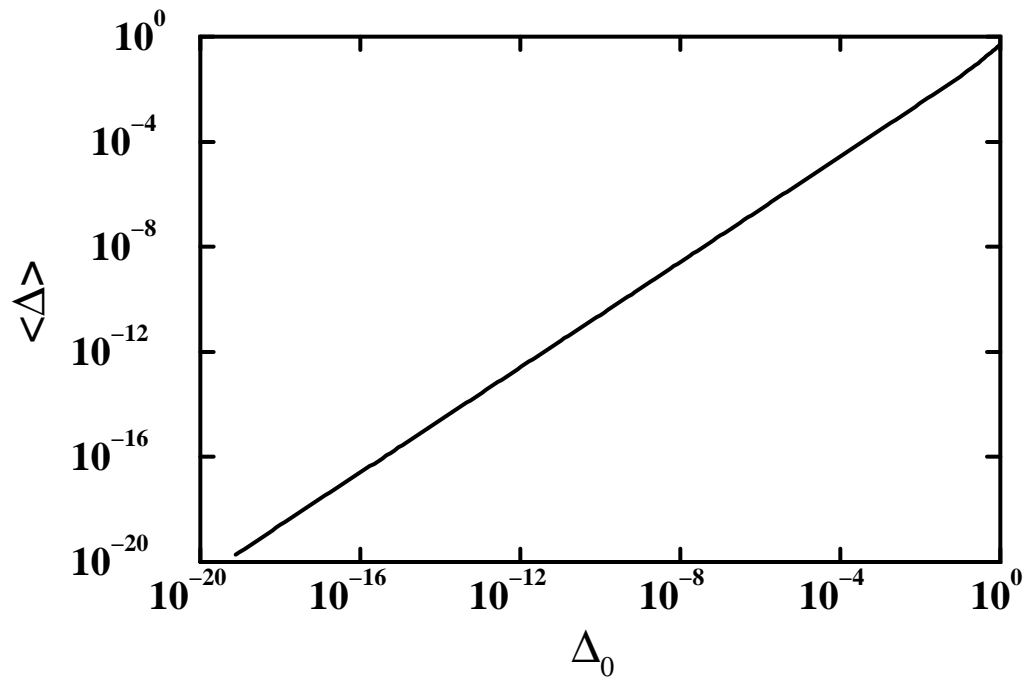


Figure 4 in the article "The low-energy fixed points of random quantum spin chains" by E. Westerberg, A. Furusaki, M. Sigrist, and P. A. Lee.

(a)



(b)

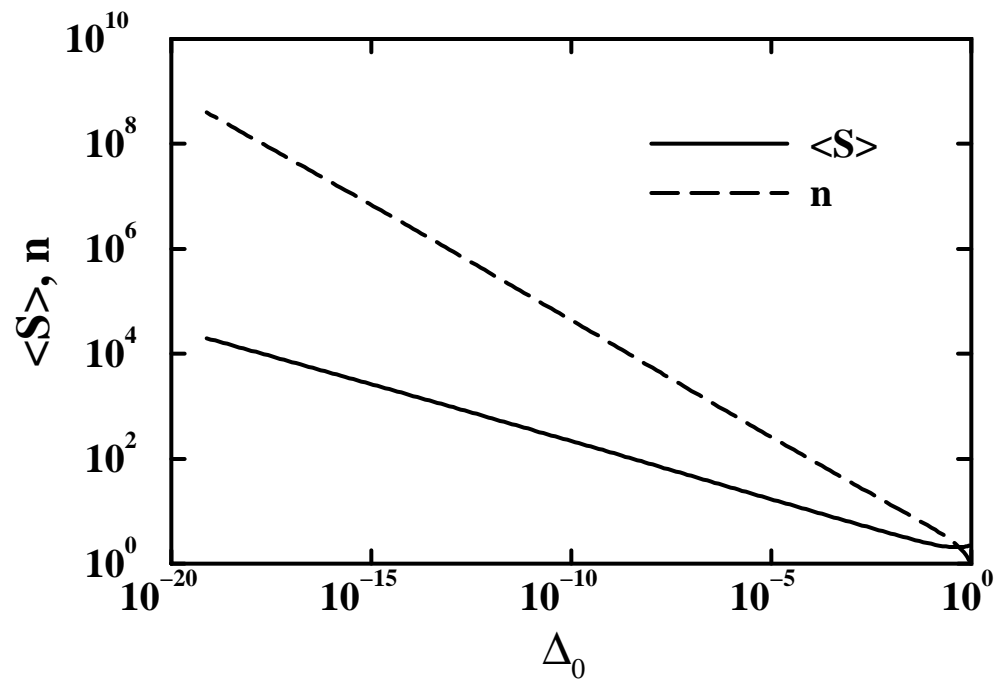
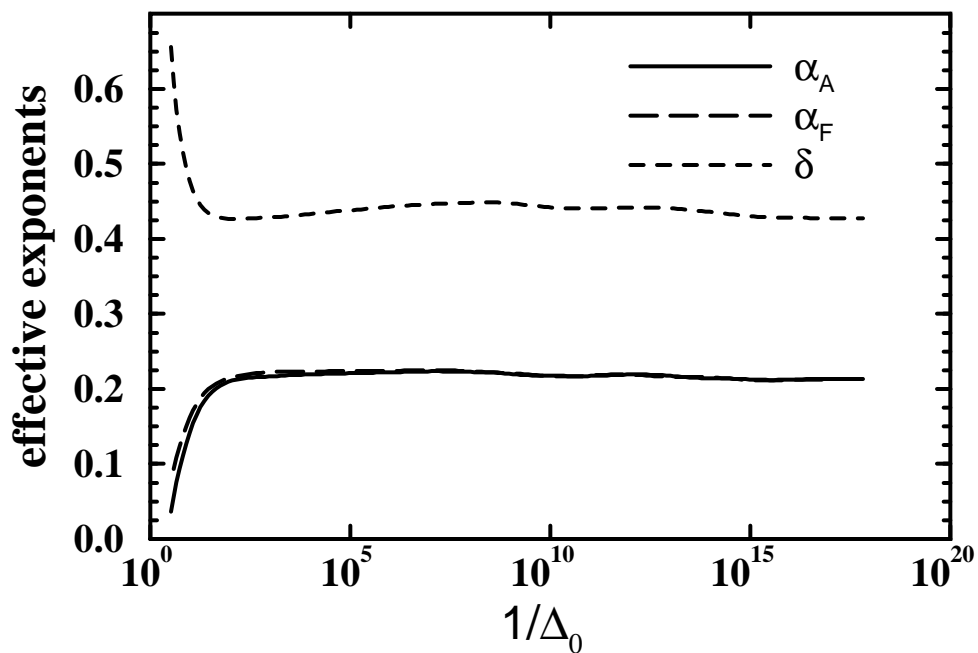


Figure 5 in the article "The low-energy fixed points of random quantum spin chains" by E. Westerberg, A. Furusaki, M. Sigrist, and P. A. Lee.

(a)



(b)

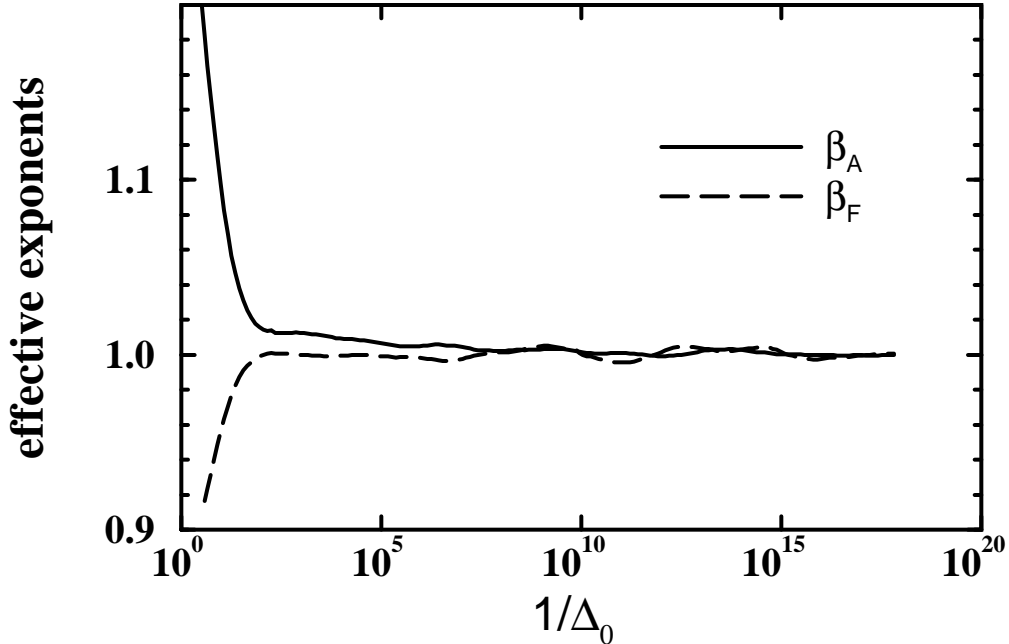


Figure 6 in the article "The low-energy fixed points of random quantum spin chains" by E. Westerberg, A. Furusaki, M. Sigrist, and P. A. Lee.

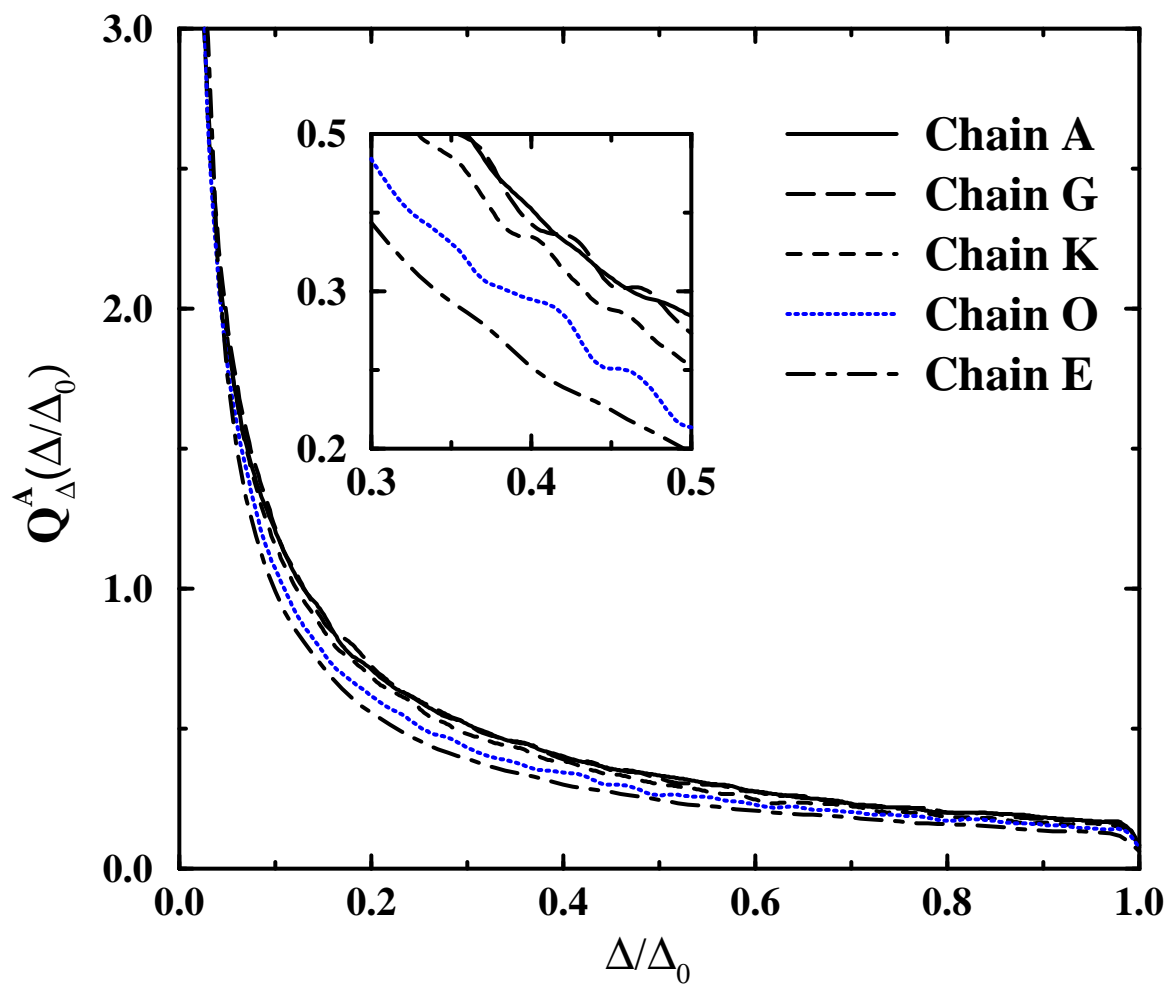
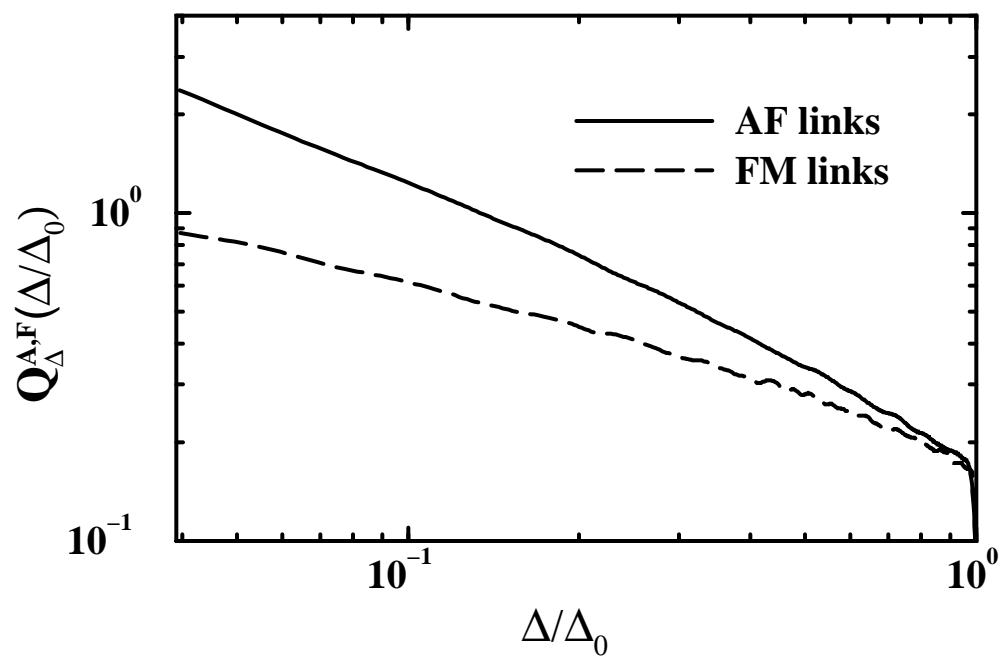
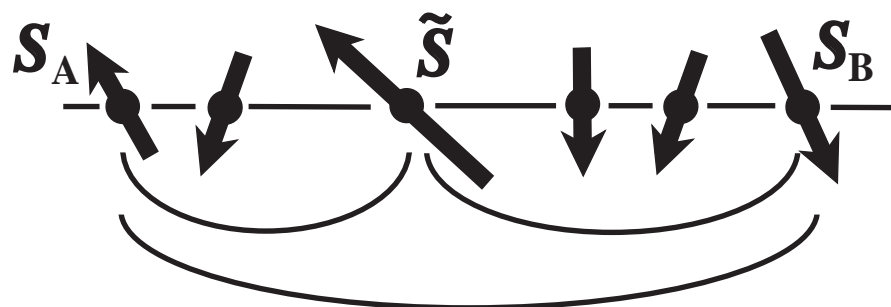
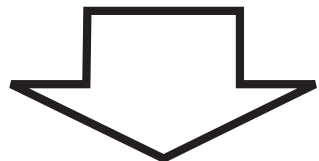
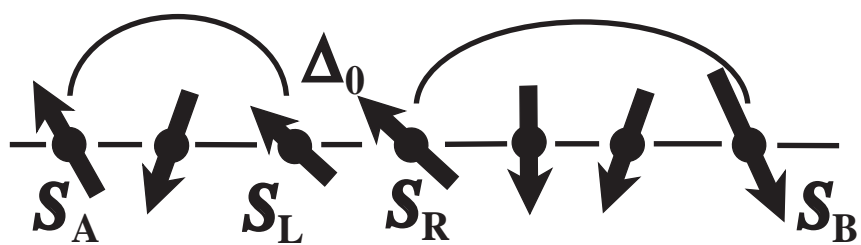
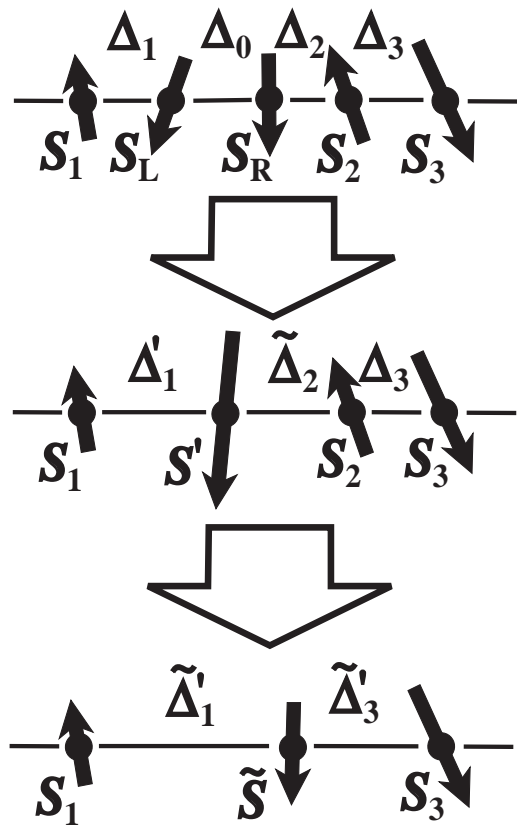


Figure 7 in the article "The low-energy fixed points of random quantum spin chains" by E. Westerberg, A. Furusaki, M. Sigrist, and P. A. Lee.





(a)



(b)

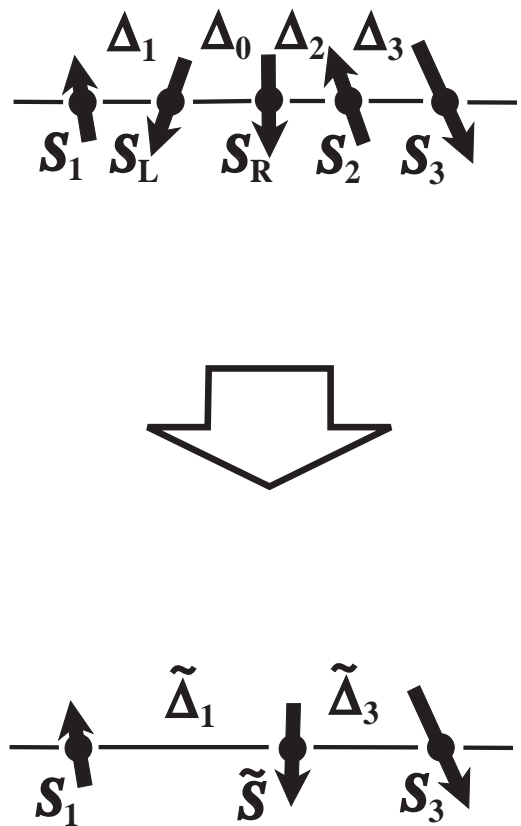


Figure 10 in the article "The Low-Energy Fixed Points of Random Quantum Spin Chains" by E. Westerberg, A. Furusaki, M. Sigrist, and P. A. Lee

